Response to Reviewers' comments on Wilson et al., "Can organic matter flux profiles be diagnosed using remineralisation rates derived from observed tracers and modelled ocean transport rates?"

We would like to thank both reviewers for their constructive feedback. We have addressed all the comments in a revised manuscript which are described below and have also restructured the manuscript in response to comments from both reviewers. The reviewer comments below are shown in bold and are followed by our response with details of specific changes made to the text where appropriate.

Response to Anonymous Referee #1:

Specific Comments:

1: (Section 2) I find the description of time stepping and time-scales associated with the inversion and diagnosed ISS a bit confusing – what is the unit of dt? Alternatively: what is the time step length for the construction of GENIE's TM? This also relates to the colour scales of figures.

We thank the reviewer for highlighting this as an issue. The units dt^{-1} are intended to reflect the remineralisation rate calculated over the model timestep. Our original intention to use this unit was to keep a focus on the fact that remineralisation rate estimates are a quantity dependent on the ocean circulation model. We have taken on board comments from both reviewers on this and have changed the units to $year^{-1}$ throughout the manuscript as we agree that this is a much clearer unit for interpretation. We have also added a clearer statement of the timestep to the text:

"The length of the time step at which the TM is diagnosed in GENIE is 0.01 year."

2: (Section 2.1) What was the reason for choosing the different locations at which the model was evaluated? Are there data sets to compare the simulated remineralisation rates (or fluxes) to?

The sites were chosen somewhat arbitrarily with the intent to give a latitudinal cross section of the estimated remineralisation rates for comparison against Henson *et al.,* (2012). The profiles were chosen to display a range of solutions from those that were completely implausible (i.e., negative rates) to those that were consistent with expectations. We agree that a comparison with observations would also be useful. However, there are a number of issues with this. Given that there are a range of positive and negative values, a direct comparison against observed remineralisation rates, such as from AOUR, highlights that the estimated profiles are in error which is already highlighted by Figure 2. Equally, apparent oxygen utilisation rates will still have the spatial averaging issue highlighted in the Introduction, which would add another level of uncertainty or require the averaging of estimated rates over large regions which is difficult due to the range of negative and positive values which average to very small near-zero values.

In response to the reviewer's comment, we have added a new panel to Figure 2 showing values of 'b' for a Martin Curve power-law function fitted to the estimated remineralisation rates using the method introduced and used later in the manuscript for the discussion of DOM remineralisation. The global mean value for 'b' is -0.90, which is within the range of previous global values found by both data and modelling studies, e.g., Kwon & Primeau (2006); Henson *et al.* (2012). However, the range of fitted values is relatively large (±2.65 1 SD) showing that some flux curves unrealistically increase with depth. The added panel also provides a complete example of the method to estimate remineralisation rates and infer flux curves. This helps to define the scope of the manuscript and complements the discussion of uncertainties from other sources of remineralisation such as DOM later in the manuscript:

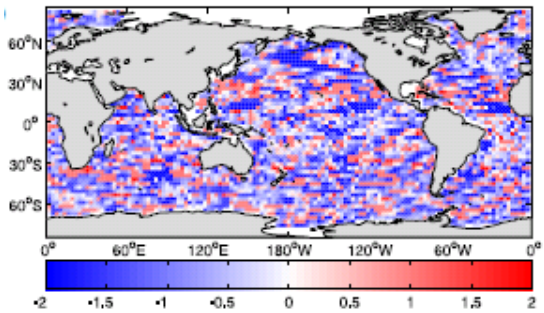

Figure 2c: Power law flux curve exponents 2b inferred from the estimated remineralisation rates by fitting a linear function to the log transformed data as in Fig. 1b.

3: (Section 2.1) "This example shows that a simple inversion of [PO4] observations using this approach is susceptible to large errors that will likely hinder their interpretation" – this is somehow vague. Is this only related to the MITgcm circulation? The fact that there is no clear pattern for ISS in 2000m when the MITgcm TM is used together with observations, but there seems to be a pattern for the GENIE TM, when diagnosed with the synthetic data set to me is a bit puzzling. Wouldn't it be interesting, to have the same comparison (TM with PO4 observations, as for MITgcm) for the GENIE TM?

This is intended to refer to the use of any TM, not just the MITgcm. We have clarified this statement in the text as follows:

"The negative ISSs and positive values for b suggest that the simple inversion of [PO_4] observations using this approach is susceptible to large errors that warrant further analysis to characterise and quantify potential uncertainties with this method when used with any modelled circulation."

In reference to the pattern observed for the synthetic data, the TM in the initial submission included the effects of virtual salinity fluxes to account for the effects of dilution/concentration on fixed volume grid-boxes caused by precipitation and evaporation at the surface (Edwards and Marsh 2005; Ridgwell *et al.,* 2007). This leads to the spatial patterns referred to by the reviewer in Fig. 4e and 4f as well as the minor deviations from the 1:1 line in Fig. 4a. This can be accounted for by normalising a tracer concentration before multiplication with the TM and converting the ISS back (as per the approach used for biogeochemical tracers in GENIE: Ridgwell *et al.,* 2007). This removes the minor deviations to the 1:1 line and removes the spatial patterns in Fig. 4e and 4f. As the magnitude of this effect is relatively small compared to the errors found in the manuscript, this does not change the results of the manuscript. All results in this revision have been altered to take this into account. We have added a description of this to the text:

"The TM diagnosed here includes the effects of virtual salinity fluxes applied in the ocean model to account for changes in volume (Edwards & Marsh 2005; Ridgwell *et al.,* 2007). To account for this, all tracer concentrations multiplied by the TM are first normalised by salinity and converted back to a concentration afterwards (Ridgwell *et al.,* 2007)."

We have not included remineralisation rates estimated using GENIE and observed [PO_4] as we feel this would detract from the use of GENIE as a model test of the method. We have retitled this section as "Uncertainty Analysis" to clarify the use of GENIE in the manuscript.

4: (Section 3) The biogeochemical model description could be more comprehensive, and easier to find; currently it is described under the (rather vague) title "Experiment design". In particular, I think

the description of particle sinking and remineralisation, as well as the DOM remineralisation (I assume it is a first order process) could be briefly explained, and the parameters should be given here as well. This will help the reader to put the results (remineralisation vs. circulation) into perspective, without having to look up another paper.

We have removed the "Experiment design" subtitle and have added a brief description of the biogeochemical in the text:

"In this, nutrients in the surface grid-boxes are utilised by biological activity limited by [PO_4] according to a Michaelis-Menton type limitation (a maximum rate of 1.96 μmol kg^{-1} and half saturation constant of 0.22 μmol kg^{-1}) and the ambient light levels (a linear limitation term). A fixed fraction of the uptake 66% is exported from the surface as DOM which can be transported by circulation and remineralised with a time constant of 1/0.5 year."

5: (Section 3) Were there (large) differences between the online and offline (i.e., TM) version of GENIE?

There were no large differences between the online circulation and that diagnosed in the TM, as shown by reproducing the remineralisation field. We note that the TM is not being used to run the model, only invert tracer fields.

6: (Section 3.3.2) ERR-OBS: As far as I understand, WOA (1x1 degree annual mean?) was regridded onto the (rather coarse) GENIE grid. How were the SDs calculated? Are these from WOA, then averaged onto the coarse grid? Or does the calculation of SD include both the SD from the WOA, as well as the variance due to regridding (e.g., Kriest et al., 2010).

We thank the reviewer for helping to clarify this point. The SDs reflect the SD of the WOA observations which were then regridded onto the coarser GENIE grid. In response to reviewer #2's comments, this has been changed to the standard error (SE) but still reflects the standard error of the WOA observations that are then regridded onto the GENIE grid. As such, the SEs we use reflect only uncertainty in the creation of the climatology from observations and not from the subsequent regridding to the GENIE grid. We have amended the text to make this clearer:

"We do not consider any additional uncertainty here that may arise through the re-gridding process, i.e. Kriest *et al.,* (2010)."

7: (Section 4.1) p. 4568. Why have a section (4.1) with only one subsubsection (4.1.1)? I would suggest to have either two subsubsections (e.g., "4.1.1. Results from the GENIE online model" then "4.2.2 Twin experiment"), or to combine everything into a single subsection.

We have restructured this section and have removed the spurious subsubsections.

8: (Section 4.2.1) See above, comment for section (3.3.2); where does the variability in the observations come from: WOA, regridding, or both?

As well as responding to the previous comment (6), we have removed some of the text in this section that might suggest the uncertainty from the re-gridding process is also considered:

Removed text –" as well as re-gridding the observations onto a model grid such as GENIE or MITGCM."

9: (Section 4.2.1) p. 4570, line 8: "distributions" to me sounds a bit misleading; what about "clusters"?

We agree and have changed "distributions" to "clusters"

"However, two clusters can be broadly defined in Fig 5c both with separate linear trends that correspond well with the size of the ``flux out'' term of the TM (see Table 1)."

10: (Section 4.2.1) p. 4570, line 11: What is "1-A"?

We thank the reviewer for highlighting, this is a mistake and should read (A-I), as in equation 3 of the original manuscript. This has been corrected in the text.

11: (Section 4.2.1) p. 4570, lines 12-13: "This suggests that the ISS uncertainty is a function of the way the TM is constructed." – I am having difficulties to understand this reasoning. Assuming there is only little transport (even in the online model), but variability of observations in large, wouldn't this result in the same pattern?

Figure 5c shows that the magnitude of uncertainty increases linearly with the magnitude of the uncertainty in the observations, *i.e.*, that ISSs generated from observations with large uncertainty also have relatively higher uncertainty. It also shows a cluster of ISSs that increase linearly but by a greater amount. This cluster occurs where circulation fluxes are larger in the model, as indicated by the colour scale. Effectively, this means the residence time of tracer in these grid-boxes is much smaller, *i.e.*, there is a bigger throughput of PO_4 associated with circulation during the model time-step. Commonly this occurs where convection occurs in the model as this is where those fluxes are largest. Therefore, if the magnitude of uncertainty of observations was fixed across all grid boxes, this effect of the TM would still lead to greater uncertainty in the ISSs in certain grid-boxes. As such, this is a caveat related to the TM and not the observations.

We have amended the text to make this clearer. We have also removed the trend lines from Figure 5c as these detract from the main interpretation, have amended the colour scale to reflect a "flux out" term, and have added a panel to Figure 5 to demonstrate where these grid-boxes occur:

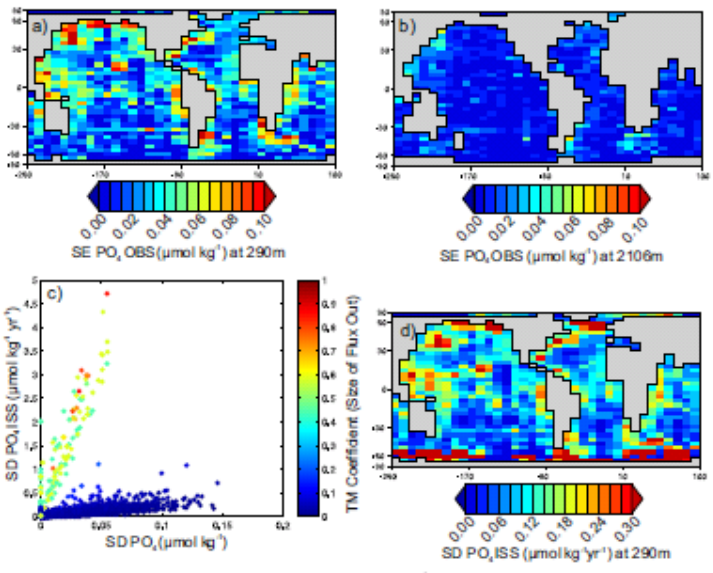

Figure 5: Assessment of the errors arising from the uncertainty in $[PO_4]$ observations. (a) The SE of $[PO_4]$ from the World Ocean Atlas 2009 (Garcia et al., 2010) 1° climatology regridded to the GENIE grid at 290m and (b) 2106m. (c) SD of all PO_4 interior source/sink estimates when the synthetic $[PO_4]$ field is randomly perturbed within a normal distribution given by the SE of observations. The colour scale indicates the size of the `flux out' term where a larger value indicates relatively larger circulation fluxes in that grid-box, (d) The SD of $[PO_4]$ ISSs at 290m.}

"This suggests that the ISS uncertainty is partly a function of the circulation diagnosed in the TM, i.e., if the observation uncertainty were fixed to a constant across all grid-boxes, ISSs in some grid-boxes will have greater uncertainty than others due to this effect."

12: (Section 4.2.2), p. 4571: I may have missed an important point, but here it is not clear to me why physical transport of the online model is related to the diagnosed (ISS) remineralisation. In particular, as far as I understand eq.3 assumes that physical fluxes in/out of each box should equal remineralisation. If this is correct, doesn't remineralisation/(online physical transport) of only about 0.001 imply that the TM constructed is very different to the online circulation?

W report the remineralisation rate as a proportion of the flux of PO_4 into the grid box. The reviewer is correct in their assertion that physical fluxes into the box minus physical fluxes out of each box should equal the remineralisation term at steady state, but here we are only considering the physical flux in term. We have added a clarification of this to the text:

"To illustrate this, we compare the steady state circulation flux of PO_4 into a grid-box with the remineralisation flux of PO_4 into each grid-box from the synthetic run (the sum of these at steady state will equal the flux of PO_4 out of the box)."

13: (Section 4.2.3) A plot of the error distribution would be interesting, and help to better understand the reason for distinguishing between median and mean.

We agree with the reviewer that this would help. As this requires displaying the error distribution for each depth level requiring a large number of panels we have added two plots to the supplementary material showing the distribution of data in Figure 8 for each depth level with the mean and median indicated for both the uncertainties from the observations and circulation.

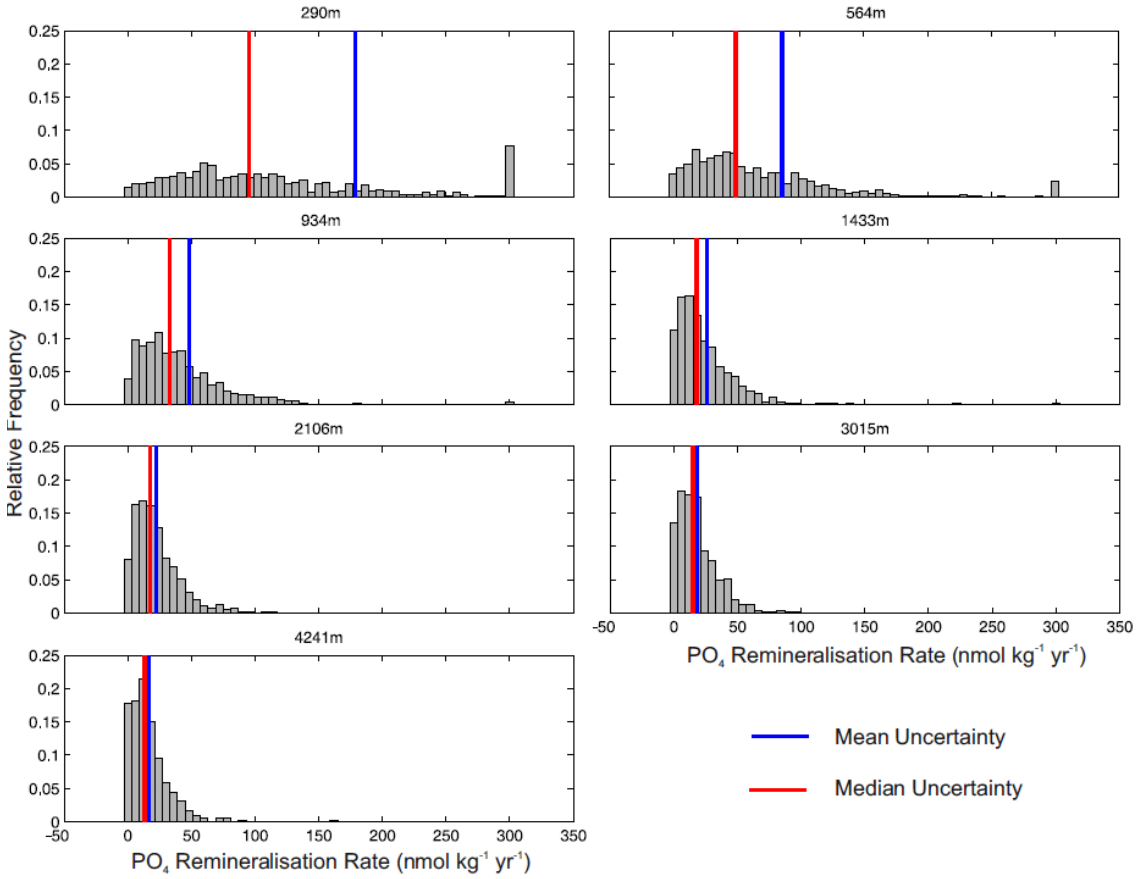

Supplementary Figure 2: Histograms showing the distribution, mean and median standard deviation of estimated PO_4 remineralisation rates when simulating uncertainty associated with observations as shown in Figure 8 for each depth level in GENIE. The histograms show the distribution standard deviations calculated for all grid-boxes at that depth level when observation uncertainty is simulated. The blue and red lines indicate the mean and median respectively corresponding with the values shown in Figure 8. Histograms are shown with a relative frequency as the number of samples is different between depth levels. Values > 300 nmol kg^{-1} yr^{-1} are included in the last bin.

14: (Section 4.2.3) p. 4572, line 9-12: "The patterns in the surface PO4 ISSs from the MITGCM inversion are systematic which may suggest that errors are predominantly related to the ocean model (Fig 2a) although this is less the case for the deeper ocean (Fig. 2b)" – How do the surface PO4 patterns (Fig 2a?) point towards errors caused by the MITgcm?

We thank the reviewer for highlighting this. We are referring to systematic features that appear in Figure 2, such as the large estimated remineralisation rates in the Southern Ocean. However, our results show this could be related to both observational and model circulation error. We have amended the text to reflect this:

"Although the patterns in the surface PO_4 ISSs from the MITgcm inversion are systematic (patches of positive and negative ISSs in the Southern Ocean: Fig 2a) it is difficult to tell whether this reflects a systematic difference between observed and modelled circulation rates, or a caveat associated with convection in the model and larger circulation fluxes in these area"

(Section 5) I find this section potentially very useful; however, discussing this before the background of remineralisation rates of DOM and POM used in the online GCM may be even more elucidating.

We have moved this section to form part of the discussion so that the uncertainty from DOM is presented and discussed in full. We have also expanded on this in the introduction. We hope this provides a more logical structure of the manuscript.

16: (Section 5) Why have a subsection 5.1 if there is not subsection 5.2?

We have removed subsection 5.1 and have restructured the manuscript.

17: (Section 5.1) page 4572, line 24: "which is converted to a flux curve by adding 1 (Stanley et al., 2012; …" – The relation between flux and remineralisation was already noted by Martin et al., (1987; their eqn.7), so I suggest to cite their paper.

The reviewer is correct that Martin et al., (1987) noted and used this method. Our use of Stanley et al., (2012) is due to their application to estimated rates derived directly from tracer observations whereas Martin *et al.,* (1987) applied this to sediment trap observations of particulate fluxes. We have added Martin *et al.,* (1987) to the text.

18: (Section 5.1) page 4573, lines 10-11: I cannot follow the authors' conclusion "The DOM bias in GENIE occurs predominantly in the high latitudes where DOM is efficiently advected into the ocean interior". – If DOM was advected deep in the ocean, where it then (quickly?) remineraliased, deep convection in the Southern ocean should result in steeper flux profiles, i.e., higher flux exponents (e.g., closer to -0.5).

We thank the reviewer for highlighting this and agree with their point. Figure 9b does show this occurring in a few water columns in the North Atlantic where the fitted values of 'b' actually increase (a deepening of the flux curve). This is consistent with convection in the model in that region. Here, DOM is efficiently advected into the ocean interior and remineralised deeper than in other regions, such as in the Southern Ocean. The uncertainty created from DOM does not, therefore, always lead to a shallower bias in estimated flux curves. We have amended the text to reflect this as follows:

"In a few grid-boxes in the North Atlantic the estimate of the flux curve exponent increases. This has a strong correspondence with the deepest convection (Figure 3.4f) where DOM is transported deeper into the water column before remineralisation. This highlights that an additional source of remineralisation not restricted to vertical processes can alter the flux curve in an unpredictable way."

19: (Section 6) p 4573, lines 21-22: not everyone would call a 2.8x2.8 degree model a "high resolution model".

We agree with the reviewer and have removed "high resolution".

20: **(Section 6) p 4574, line 3-6: "Previous methods have relied on relating multiple tracers together such that the model transport 5 terms cancel out, e.g. Anderson and Sarmiento (1994); Sarmiento et al., (2002) and is a method which could be applied using the TM." – what is the meaning of this sentence?**

Specifically, estimates of remineralisation rates could be derived from $[PO_4]$ and $[NO_3]$ for example, on the assumption that the error from the model circulation will cancel out. On consideration of the reviewer's comment, we have removed this from the discussion.

21: (Section 6) The assessment of circulation-based error via salinity could be in a separate subsection.

We have added an additional subsection in the discussion to discuss the constraints on the circulation uncertainty.

22: (Section 6) The meaning of the last few sentences to is quite unclear. I would strongly suggest some more in depth discussion of the results of the present study before the background of other model studies: for example, Kwon and Primeau could constrain b of a very simple model from PO4 data (without having spinup the model thousands of years). Their model also included DOM, and they provided constraints for its production and decay parameters. Decades, ago, Bacastow and Maier-Reminer (1991) set up models similar to the one used in this study, and carried out experiments with different sinking speeds and DOM/no DOM. Finally, DOM, in its role in the regulations of nutrient fields, and its interplay with circulation has a long "history" in modelling, and this has been examined in many studies (e.g., Najjar etal., 2007).

We have restructured this section to explicitly first consider the results of the manuscript before then discussing further work with a more detailed description and expanded citations.

23: Table 1 and its caption – please explain, why there are 8 boxes. "The amount in italics is the estimated remineralisation" – is this number in the lower right corner?

Typically there are 15 grid-boxes for each column of the GENIE TM, reflecting dye travelling to neighbouring grid-boxes above/below, to the east/west and north/south as well as neighbouring grid-boxes on the vertices due to the Gent-McWilliams parameterisation. The number of grid-boxes is either reduced where there is a boundary, e.g., the surface or sediment, or increased where there is convection. The 8 grid-boxes in Table 1 were intended to show a reduced version, but in hindsight as the reviewer alludes to, this is not clear.

In response we have reduced the example in Table 1 to 7 boxes, i.e., a central box and 6 neighbours and have included this in the caption text. We have also labelled each box with compass direction relative to the central box to help clarify the example. This also facilitates the comparison with the TMI method (Gebbie and Huybers 2010) in the discussion:

Table 1: Example of using a transport matrix to calculate PO_4 remineralisation (mol kg^{-1} yr^{-1}) in one grid-box from PO_4 concentrations (mol kg^{-1}) given in **c**. Grid-boxes, taken from a row of the TM, are arbitrarily numbered, where the 1 is the central grid-box where the calculation is taking place. The example shows a simplified situation where there are 6 neighbouring grid-boxes with their relation to the central grid-box given by the directions in brackets. Each coefficient in the 6 boxes represents the flux of PO_4 into the central box from that grid-box. The coefficient in the central grid-box for **A** (see Eq. 1) represents the amount of tracer left in the central grid-box after one timestep whilst the

Grid-Box	**A**	$(\mathbf{A}-\mathbf{I})$	c
1 ('flux out')	0.9816	−0.0184	2.3439
2 ('north')	−0.0007	−0.0007	2.3430
3 ('south')	0.0086	0.0086	2.4334
4 ('east')	0.0002	0.0002	2.3529
5 ('west')	0.0005	0.0005	2.3615
6 ('above')	0.0097	0.0097	2.4433
7 ('below')	0.0001	0.0001	2.3369
	1.0000	0.0000	**0.0011**

coefficient for **A-I** (see Eq. 2) is the flux out, equal to 0.9816-1. The sum of coefficients is shown underneath with the estimated remineralisation (**q** in Eq. 2) in bold calculated as the sum of the element wise multiplications of **A-I** and **c**.

24: Figure 1 – is depth relative to z0?

The depth scale is absolute. The plot is plotted on the MITgcm grid, so z0 is ~25m making it appear like depth is relative to z0 as it is close to zero. We have added a reference to this in the caption of Figure 1.

25: Figure 2 (and other figures); Some of the panels are very small. In some figures (e.g., 2b) it the very difficult to distinguish positive from negative values. The units are difference (e.g., mmol m-3 dt-1 in Fig 2 vs nmol kg-1 dt-1 in Fig 4 and 6), making it difficult to compare the different figures. Sometimes the units on colour bar don't seem to be correct (e.g., Fig 3c,d; no time constant for flux in figure, but in caption), which is quite confusing.

We have replotted Figure 2 using a more appropriate colour scale that highlights positive vs. negative values with a white zero value. The different scales are a result of trying to show both spatial patterns, as the focus of this manuscript, and changes with depth, as we are dealing with water column remineralisation. Unfortunately, large differences in magnitude make it difficult to plot on the same scale. We have highlighted this in the figure captions where this occurs. We thank the reviewer for highlighting the units on the colour bars of Figure 3c and 3d and have amended them to match the caption.

Response to Anonymous Referee #2

General Comments:

1: In order to have a good publishable result, the authors should undertake additional work to develop this method so that it can yield robust estimates of remineralization rates.

The intended scope of our manuscript was to introduce a potential approach to exploring spatial variability in particulate organic matter fluxes estimated from remineralisation rates, and to identify and quantify the sources of error associated with this approach. Ultimately our error assessment shows that the potential errors are very large, and as the reviewer notes, our manuscript does not develop the method to the point of yielding robust estimates of remineralisation rates. Firstly, we feel that this is outside the scope of the manuscript and would warrant another manuscript to fully describe any further development. We highlighted a potential first step in accounting for the errors associated with using modelled circulation rates based on previously published methods using conservative tracers to constrain the error. However, the number of conservative tracers available would lead to an underdetermined problem, even if we applied a 7-point stencil as per Gebbie & Huybers (2010). We did look into various methods, including adding additional constraints based on the range of circulation rates in the 54 member ensemble, but found they could not reliably constrain the errors or relied heavily on assumptions. As such, we focused on identifying and quantifying the sources of error to provide a resource for future work. Secondly, by maintaining a scope on quantifying errors, we can also explore uncertainties associated with using robust estimates of remineralisation rates to infer flux profiles, e.g., Martin *et al.,* (1987) and Stanley *et al.,* (2012). Ultimately, our analysis suggests that even with robust estimates, there are still significant uncertainties that will affect the interpretation of flux curves. This makes the manuscript relevant to a wider range of studies, including those that are observation based, and also highlights other approaches such as optimising ocean biogeochemical models are an important next step.

We have extended the discussion of the limitations to constraining the sources of error identified in the manuscript as well as restructuring the manuscript in line with other comments from both reviewers to clarify the scope of the manuscript.

2: Many similar "inverse" models that have been developed and applied successfully to elucidate aspects of the ocean's biological pump functioning (some cited in this paper and others not).

There are inverse approaches that we have not touched on in this manuscript. Notably, there are a number of studies that describe the biological pump function in a model and fit values to infer aspects of the biological pump, e.g., Schlitzer *et al.,* (2002); Kwon and Primeau (2006); Kriest *et al.* (2012); Yao and Schlitzer (2013). As per the response to **(1)**, we have tried to maintain a focus on directly estimating remineralisation rates in order to infer particulate organic matter flux curves. We have expanded the discussion with additional citations to better describe potential alternatives to the method we have presented and how they are related to each other to help stimulate further developments in this area.

3: The TMI method has been used to determine rates of mass transport as well, using radiocarbon data (Gebbie and Huybers, 2011).

We have added this citation to the text:

"This is because the TMI method reflects the pathways of ocean transport but not the rates of transport Gebbie & Huybers (2010), although Gebbie & Huybers (2012) additional information concerning rates can be estimated when combining the TMI method with radiocarbon data.

4: equation 1: The equation appears to be wrong. The authors don't state the units of A (which are typically dtˆ-1), but there are no units of A that could make the equation correct because c has units of (mol kgˆ-1) and q has units of (mol kg dtˆ-1). So the units on the left-hand side and right-hand side are not the same. If the units of A are dtˆ-1, the correct equation is dc/dt = A*c + q. Page 4563, equations 2 and 3. Again, appears not to be correct (see above). For (3) it should be q = -A*c.

We thank for the reviewer for highlighting the inconsistency between the equations and the units. Equation 1 corresponds to equation (2) in Khatiwala (2007) for the discretised advection-diffusion equation. In the method of Khatiwala et al. (2005), the finite difference tendency is calculated from a model:

$$\frac{d\mathbf{c}}{dt} = \frac{\mathbf{c}^{n+1} - \mathbf{c}^{n}}{\Delta t} = \mathbf{A}'^{n}\mathbf{c}^{n} + \mathbf{q}'^{n}$$

for which the units given for **q** in the manuscript (mol kg^{-1} dt^{-1}) would be correct, and as the reviewer highlights the units of **A'** will be dt^{-1}. Equation (1) of the manuscript is derived by rearranging the above equation for $\boldsymbol{c}^{n+1}$:

$$\mathbf{c}^{\mathrm{n}+1} = (\mathbf{I} + \mathbf{A}'\Delta t)\mathbf{c}^{n} + \mathbf{q}'^{\mathrm{n}}\Delta t$$

In our manuscript, we do not diagnose the finite difference tendency in GENIE, just the tracer distribution resulting a unit flux at the next time step so our matrix $\mathbf{A}$=$(\mathbf{I} + \mathbf{A}'\Delta t)$. $\mathbf{A}$ is now unitless, and the source/sink term ($\mathbf{q} = \mathbf{q}'^{\boldsymbol{n}}\Delta \boldsymbol{t}$) is mol kg^{-1}. This is now the equation in form given by Khatiwala (2007). Therefore, the units stated in the manuscript are not correct and should mol kg^{-1} for $\mathbf{q}$.

Rearranging equation (1) in the manuscript for **q**, assuming for steady state that $\mathbf{c}$=$\mathbf{c}^{n+1}$=$\mathbf{c}^{n}$, i.e., the tracer concentration does not evolve through time, gives:

$$\mathbf{q} = (\mathbf{A} - \mathbf{I})\mathbf{c}$$

The coefficients in matrix $\mathbf{A}$ can be conceptually understood as mapping how the tracer concentration at any one point on the model grid changes due to the net effect of model circulation during one timestep. $(\mathbf{A} - \mathbf{I})$ can be conceptually understood as calculating the net change in a tracer due to the model circulation in one timestep. We have added this to the supplementary material.

5: Figure 1: (a) Labeling one curve as high-latitude and one as low-latitude is a bit misleading, since these are not based on actual data, and the differences in observed particle flux attenuation from high-lat vs. low-lat regions is not so cut and dry. (b) is impossible to interpret due to x-axis scale. c) Is this just a repeat of (b) on a log scale?

We thank for the reviewer for this feedback. We have removed panel b from Figure 1 leaving only the remineralisation rate profiles on a log scale. This complements the description of the method and Introduction. We have also removed the profiles from Figure 2 in light of this feedback and have replaced it with a map of fitted 'b' values derived from the estimated remineralisation rates. This facilitates a more direct comparison with previous studies and avoids complications when referring to high/low latitudes.

6: Figure 2: c) Again very hard to interpret because of scales

Please see response to **(5)**.

7: Figure 3 f) How is the cost function defined?

The cost function is the average of number of grid-boxes in each water column that are mixed by convection. Higher values indicate deeper convection on average. We have changed the figure caption to reflect this.

8: Figure 5 and associated discussion: The use of random errors for the PO4 field is not appropriate here. The errors are significantly spatially correlated – which probably has important implications for inferring the remineralization flux. It would also be more appropriate to use the standard error, rather than the SD.

We have replaced the standard deviation of the observations with the standard error. The errors are intended to be illustrative but spatially correlated errors will need to be considered for future work. We thank the reviewers for highlighting the issue of spatially correlated errors and have added this to the text:

"We note that errors in the observations may be spatially correlated which will warrant consideration in future work."

9: Figure 5 and throughout: Should replace mol kgˆ-1 dtˆ-1 with something interpretable (like mol kgˆ-1 yrˆ-1)

We have replotted all figures with units of yr^{-1}.

10: Figure 5: Hard to tell how large the error in the diagnosed ISS are relative to the actual ISS

The errors are generally much larger than the diagnosed ISSs such that plotting relative standard deviation to highlight the relative error size makes it difficult to highlight the effect of coefficients on the diagnosed ISSs. A comparison of the size of errors versus the ISSs can be seen in Figure 8. We have therefore kept Figure 5c but have added a description of the size of the errors to the text:

"The resulting variability in the PO_4 ISSs, as characterised by the SD, are relatively large compared to the ISS values themselves, around 1--3 orders of magnitude larger than the ISS values (see also Fig. 8)."

11: Page 4571, lines 16-18. The authors identify exactly the problem with this approach. So there needs to be some way to move beyond or modify this point-by-point approach

Please see response to **(1)**

12: Page 4572, line 10 ff. The pattern of ISS in fig. 2 probably appears relatively smooth because the smooth mapped observations were used.

We thank the reviewer for highlighting this. The smooth mapped observations are used because missing data values will be propagated by the transport matrix resulting in a sparse number of remineralisation estimates. We have added this point to the manuscript:

"The relative smoothness of the ISS estimates may reflect the use of the climatology which has already been smoothed (Garcia *et al.,* 2010)."

13: Section 5.1 This is an interesting section showing the effect of DOM on the inferred particle flux profiles. However, it's a bit out of place here because the particle flux profiles cannot be diagnosed using the method the authors present.

We feel that a discussion of DOM, or more generally sources/sinks that are not restricted to the vertical water column, is still relevant to the scope of the manuscript. We are aware of papers that have used remineralisation rate profiles to infer particulate flux curves, e.g., Feely *et al.,* (2004); Stanley *et al.,* (2012); Sonnerup *et al.,* (2013), but there has not been an assessment of this particular uncertainty. Given that the manuscript focuses on moving on from the AOUR approach to estimate the spatial patterns in particulate organic matter fluxes, the uncertainty from integrating remineralisation rates vertically we feel that this fits within the scope of the study. We have restructured the manuscript to better reflect its scope.

14: Page 4573, line 21: coarse resolution ocean model

The MITgcm is a high resolution model in comparison to GENIE, we have amended the text in the manuscript to reflect this:

"…in an example inversion using a circulation field from a coarse resolution ocean model"

15: l Section 6: This section presents some interesting ideas, but unfortunately none are followed through on.

Please see response to **(1)**

16: Page 4575, line 10 ff. The method of Gebbie and Huybers is basically exactly this. They just adopt a 7-point stencil for fluxes between boxes so that the problem can be solved.

We have added this to the text:

"It would be interesting to see if a simplified TM with fewer coefficients, such as matching the method of Gebbie & Huybers (2010) by adopting a 7-point stencil, could use this approach"

17: Figure 8: I found this to be an odd way to represent these results. Also it is very hard to see the PO4 remineralization rate on this scale

We have expanded the discussion of the figure to reflect specific examples and to clarify that we do not expect a strong correspondence between the two:

"Comparing the errors from the inversion of the synthetic [PO_4] field using the same TM shows that the two have some visible similarities (Fig. 9e and f). For example, there are correspondences in the deep South Atlantic (Fig. 9d and e) and the subtropical regions of the Pacific at 290m (Fig. 9c and e). We do not expect an exact correspondence but the visual similarities support the idea that they are related via errors in the model circulation."

References

Buesseler, K.O., *et al.,* (2007) An assessment of the use of sediment traps for estimating upper ocean particle fluxes. *Journal of Marine Research.* 65 (3), pp. 345 - 416

Edwards, N., and R. Marsh (2005), Uncertainties due to transport-parameter sensitivity in an efficient 3-D ocean-climate model, *Climate Dynamics*, 24 (4), 415-433.

Garcia, H., R. Locarnini, T. Boyer, J. Antonov, M. Zweng, O. Baranova, and D. Johnson (2010), World Ocean Atlas 2009, Volume 4: Nutrients (phosphate, nitrate, silicate)., in NOAA Atlas NESDIS 71, edited by S. Levitus, U.S. Government Printing Office, Washington, D.C.

Gebbie, G., and P. Huybers (2010), Total Matrix Intercomparison: A method for determining the geometry of water-mass pathways, *Journal of Physical Oceanography*, 40 (8), 1710-1728, doi:10.1175/2010JPO4272.1.

Gebbie, G., and Huybers, P., (2012) The mean age of ocean waters inferred from radiocarbon observations: sensitivity to surface sources and accounting for mixing histories. *Journal of Physical Oceanography.* 42 (2), pp. 291-305

Henson, S., R. Sanders, and E. Madsen (2012), Global patterns in efficiency of particulate organic carbon export and transfer to the deep ocean, *Global Biogeochemical Cycles*, 26, GB1028, doi:10.1029/2011GB004099.

Khatiwala, S., M. Visbeck, and M. A. Cane (2005), Accelerated simulation of passive tracers in ocean circulation models, *Ocean Modelling*, 9 (1), 51 { 69, doi:http://dx.doi.org/10.1016/j.ocemod.2004.04.002.

Khatiwala, S. (2007), A computational framework for simulation of biogeochemical tracers in the ocean, *Global Biogeochemical Cycles*, 21 (3), GB3001, doi:10.1029/2007GB002923.

Kriest, I., A. Oschlies, and S. Khatiwala (2012), Sensitivity analysis of simple global marine biogeochemical models, *Global Biogeochemical Cycles*, 26 (2), GB2029, doi:10.1029/2011GB004072.

Kwon, E. Y., and F. Primeau (2006), Optimization and sensitivity study of a biogeochemistry ocean model using an implicit solver and in situ phosphate data, *Global Biogeochemical Cycles*, 20 (4), GB4009, doi:10.1029/2005GB002631.

Marsay, C., R. Sanders, S. Henson, K. Pabortsava, E. Achterberg, and R. Lampitt (2015), Attenuation of sinking particulate organic carbon ux through the mesopelagic ocean, *Proceedings of the National Academy of Sciences,* 112 (4), 1089-1094, doi:10.1073/pnas.1415311112.

Ridgwell, A., J. C. Hargreaves, N. R. Edwards, J. D. Annan, T. M. Lenton, R. Marsh, A. Yool, and A. Watson (2007), Marine geochemical data assimilation in an efficient earth system model of global biogeochemical cycling, *Biogeosciences*, 4 (1), 87-104, doi:10.5194/bg-4-87-2007.

Schlitzer, R. (2002a), Carbon export fluxes in the southern ocean: results from inverse modeling and comparison with satellite-based estimates, *Deep Sea Research Part II:Topical Studies in Oceanography*, 49 (9{10), 1623 { 1644, doi:http://dx.doi.org/10.1016/S0967-0645(02)00004-8.

Sonnerup, R. E., S. Mecking, and J. L. Bullister (2013), Transit time distributionsand oxygen utilization rates in the northeast pacific ocean from chlorofluorocarbons and sulfur hexafluoride, *Deep Sea Research Part I: Oceanographic Research Papers*, 72 (0), 61-71, doi:http://dx.doi.org/10.1016/j.dsr.2012.10.013.

Stanley, R. H. R., S. C. Doney, W. J. Jenkins, and D. E. Lott III (2012), Apparent oxygen utilization rates calculated from tritium and helium-3 profiles at the bermuda atlantic time-series study site, *Biogeosciences*, 9 (6), 1969-1983, doi: 10.5194/bg-9-1969-2012.

Yao, X., and Schlizter, R., (2013) Assimilating water column and satellite data for marine export production estimation. *Geoscientific Model Development.* 6 (5), pp. 1575 – 1590, doi: 10.5194/gmd-6-1575-2013

Manuscript prepared for Biogeosciences Discuss.
with version 2014/09/16 7.15 Copernicus papers of the LaTeX class copernicus.cls.
Date: 10 July 2015

Can organic matter flux profiles be diagnosed using remineralisation rates derived from observed tracers and modelled ocean transport rates?

J. D. Wilson[1,2], A. Ridgwell[2,3], and S. Barker[1]

[1]School of Earth and Ocean Sciences, Cardiff University, Cardiff, UK
[2]School of Geographical Sciences, University of Bristol, UK
[3]Department of Earth Sciences, University of California, Riverside CA, USA

Correspondence to: J. D. Wilson (wilsonjd@cardiff.ac.uk)

Abstract

The average depth in the ocean at which the majority of sinking organic matter particles remineralise is a fundamental parameter in the oceans role in regulating atmospheric CO_2. Observed spatial patterns in sinking fluxes and relationships between the fluxes of ~~difference~~ different particles in the modern ocean have widely been used to invoke controlling mechanisms with important implications for CO_2 regulation. However, such analyses are limited by the sparse spatial sampling of the available sediment trap data. Here we explore whether model ocean circulation rates, in the form of a transport matrix, can be used to derive remineralisation rates and infer sinking particle flux curves from the much more highly resolved observations of dissolved nutrient concentrations. Initially we show an example of the method using a transport matrix from the MITgcm model and demonstrate there are a number of potential uncertainties associated with the method. We then use the Earth system model GENIE to generate a synthetic tracer dataset to explore the ~~methods~~ method and its sensitivity to key sources of uncertainty arising from errors in the tracer observations and in the model circulation. We use a ~~perturbed physics ensemble to generate~~ 54 ~~different estimates of~~ member ensemble of different but plausible estimates of the modern circulation to explore errors associated with model transport rates. We find that reconstructed remineralisation rates are ~~highly~~ very sensitive to both errors in observations and ~~our ensemble uncertainty in~~ the use of model circulation rates such that a simple inversion ~~does not provide a~~cannot provide a robust estimate of particulate flux profiles. ~~Inferred~~ Estimated remineralisation rates are particularly sensitive to differences between the ~~'observed' and modelled transport fluxes~~ "observed" and modelled circulation because remineralisation rates are ~~3-4~~ 3–4 magnitudes smaller than ~~circulation~~ transport rates. We ~~also find that~~ highlight a potential method of constraining the uncertainty associated with using modelled circulation rates although its success is limited by the observations currently available. Finally, we show that there additional uncertainties when inferring particle flux curves from ~~remineralisation rates the~~ reliable estimates of remineralisation rates due to processes that are not restricted to the vertical water column such as the cycling

of dissolved organic matteralso creates biases that have a similar magnitude and spatial variability to flux curves diagnosed using sediment trap data. We end with a discussion on the potential future directions and pitfalls of estimating remineralisation rates using model circulation schemes. .

1 Introduction

Sediment trap studies show that the vertical flux of particulate organic carbon (POC) can be described empirically by a power-law curve (e.g. the 'Martin Curve' "Martin Curve" Martin et al., 1987; see Fig. 1a) where POC is rapidly remineralised in the upper water column (<1000m< 1000 m) leaving a small fraction (5-105–10 %) of POC that sinks to greater depths. The exponent of the Martin Curve (b) reflects the distribution of POC with depth and whether POC is remineralised higher or lower in the water column. Recent studies using deep global sediment trap observations, observations of ^{234}Th fluxes and particle concentration data suggest ahave suggested a highly heterogeneous pattern of flux profiles and the existence of a general latitudinal trend (Lutz et al., 2007; Honjo et al., 2008; Lam et al., 2011; Henson et al., 2012). POC fluxes in high latitude regions decrease faster with depth, i.e. they display shallower flux curves than in low latitude regions where a greater proportion of POC is remineralised at deeper depths (Fig. 1a). These However these patterns may be biased by a focus on deep ocean fluxes however due to sampling biases in shallower traps (Buesseler et al., 2007). An anaylsis of neutrally bouyant sediment traps have since suggested shallower POC fluxes have a latitudinal pattern inverse to that found in deep traps(Marsay et al., 2015). Analysis of the POC fluxes supports a number of mechanisms that explain these spatial patterns including increased sinking velocity of particles via a 'ballast' "ballast" effect from minerals such as $CaCO_3$ $CaCO_3$ (Armstrong et al., 2002; Klaas and Archer, 2002); aggregation of particles (Passow, 2004); and surface ecosystem dynamics, such as the level of nutrient recycling and blooms altering characteristics of the particles being exported (Lam et al., 2011; Le Moigne et al., 2012; Henson et al., 2012); and temperature dependent remineralisation rates (Marsay et al., 2015). However, further

progress has been hindered by the relatively low sampling density of long-term sediment trap deployments, particularly in regions such as the Southern Ocean, e.g. Le Moigne et al. (2012); Wilson et al. (2012).

Understanding the underlying reasons for the spatial patterns in remineralisation is a valuable step in understanding mechanisms driving the biological pump. This is key to understanding how the biological pump will respond to both past and current changes in climate (Honjo et al., 2014). Atmospheric carbon dioxide (~~CO_2~~CO_2) concentrations have been shown to be sensitive to changes in flux profiles when modelled, primarily via the effect of redistributing DIC in the modern ocean interior (Kwon et al., 2009). Atmospheric ~~CO_2~~ CO_2 is also potentially sensitive to changes in the POC flux to deep-sea sediments relative to fluxes of calcium carbonate (~~$CaCO_3$~~$CaCO_3$) over longer timescales (Archer and Maier-Reimer, 1994; Roth et al., 2014). The range of potential mechanisms results in a range of potential feedbacks for the biological pump ~~of~~ with different magnitudes and directions that will respond to a range of different environmental factors. An additional source of uncertainty in modelling sensitivity studies is that only global changes in remineralisation depths, not spatially variable changes, have been considered.

A potential approach to increasing and enhancing the resolution of POC observations is to use climatological fields of dissolved nutrients to estimate POC remineralisation rates. The water column profile of remineralisation rates can be related to flux curves by the fact that the vertical profile of remineralisation rates is the first derivative of the vertical profile of fluxes, e.g. (Martin et al., 1987) (Fig.~~1a and 1~~ 1a and b). The global distribution of a biological nutrient, such as phosphate (~~PO_4~~PO_4) or dissolved inorganic carbon (DIC), results from the net action of the biological pump (uptake during photosynthesis at the ocean surface and subsequent remineralisation of organic matter in the interior) in combination with physical processes (e.g. ~~air-sea~~ air–sea gas exchange) and other biological processes (such as denitrification) that are integrated through time via ocean circulation. In particular, the concentration of Apparent Oxygen Utilisation (AOU) has a long history of use as a measure of net organic matter remineralisation in the ocean interior. When combined with a tracer tracking the age of water masses, AOU can be converted to apparent oxygen utilisation

rates (AOUR) and related to carbon remineralisation via stoichiometric ratios, e.g. Jenkins (1982). Feely et al. (2004) compiled AOUR-derived profiles of organic carbon remineralisation rates for 10 regions in the Pacific noting higher rates in the North Pacific relative to the South Pacific and similarities between regions with high rates and higher ~~$CaCO_3$~~ $CaCO_3$ fluxes. However, the in-situ AOUR of a water parcel reflects the history of remineralisation over its whole trajectory (e.g. along an isopycnal) producing an average AOUR that is biased towards shallower regions where remineralisation rates are higher. Therefore, when relating AOURs back to flux profiles by integrating them vertically, estimates are representative of large oceanic regions only, i.e. there is a high degree of spatial smoothing (Sonnerup et al., 2013; Stanley et al., 2012).

An alternative to combining AOU and age tracers is to use the spatial gradients in tracers to separate out and quantify the change in a concentration of a tracer at any point from circulation only. Spatial gradients of a tracer along the trajectory of a water mass in the ocean interior reflect mixing with other water masses and processes such as the remineralisation of organic matter. Gradient based approaches aim to solve for the effect of mixing by defining a water mass as the sum of mass fractions from different sources, e.g. Anderson and Sarmiento (1994); Broecker et al. (1998); Gebbie and Huybers (2010). A recent development of this method, the Total Matrix Intercomparison (TMI) method described by Gebbie and Huybers (2010), solves for up to 6 mass fractions for each grid-box in a ~~4x 4~~ $4° \times 4°$ resolution with 33 vertical levels using temperature, salinity, $\delta^{18}O$, and nutrients with an additional source term reflecting organic matter remineralisation. The source term is related to the nutrients using stoichiometric ratios. The TMI method therefore produces a high resolution field of remineralisation estimates. However, these terms do not reflect a rate, i.e. TMI predicts mol~~PO_4~~ PO_4 remineralised in a grid box rather than mol~~PO_4 yr^{-1}~~ PO_4 yr^{-1}. This is because the TMI method reflects the pathways of ocean transport but not the rates of transport (Gebbie and Huybers, 2010), although Gebbie and Huybers (2012) additional information concerning rates can be estimated when combining the TMI method with radiocarbon data.

Spatial gradients in tracers have also been used to diagnose export fluxes of calcium carbonate (Sarmiento et al., 2002) and opal (Sarmiento et al., 2004) from the surface. The method is based on taking the ratio between the vertical gradients of Alkalinity and Nitrate in the upper ocean, to reflect the ~~$CaCO_3$:Organic Carbon export ratio assuming a~~ratio of $CaCO_3$: Organic Carbon exported from the surface assuming a dominance of vertical gradients (Sarmiento et al., 2002). The ratio is converted to a flux using estimates of organic carbon export e.g. Henson et al. (2011). However, a model-based assessment of the method suggests that biases could occur due to the remineralisation of dissolved organic matter (DOM) and strong meridional transports that violate the assumption of processes occurring primarily in the vertical dimension (Jin et al., 2006). This highlights an additional potential issue of using remineralisation rates to infer flux curves that has not been considered by previous studies.

Ocean circulation models offer the opportunity to estimate remineralisation rates of organic matter from tracer data by exploiting the calculated modelled transport rates to account for the effects of ocean circulation on tracers. The aim of this paper is to explore the feasibility of inferring flux profiles of particulate organic matter from remineralisation rates that have been derived from observed tracers ~~. A~~ using this method. A method and example of estimating remineralisation rates using transport matrices is first introduced. We identify potential sources of error for this method. We then derive a set of model experiments that are used as a synthetic dataset with which to test the sensitivity of the approaches to various sources of error and explore potential constraints on estimates. Finally, we explore the uncertainties associated with the broader concept of inferring flux curves from remineralisation rates.

2 Estimating remineralisation rates using modelled ocean transport rates

Remineralisation rates can be calculated as the amount of tracer needed to maintain tracer observations at steady state once the effects of model ocean transport have been accounted for, i.e. transport divergence (Deutsch et al., 2007). Remineralisation rates can then

be used to estimate the vertical particulate flux curve. A practical method for this ~~approach~~ is to apply a transport matrix approach. A transport matrix, hereafter abbreviated to TM, is a representation of steady state transport rates in the form of a sparse matrix that is derived empirically from an ocean circulation model (Khatiwala et al., 2005; Khatiwala, 2007). Using a TM is akin to the fixed transport rates implied in a box model, e.g. ~~'LOSCAR'~~"LOSCAR": Zeebe (2012), but with the advantage that the rates are diagnosed from a dynamic ocean model with a much higher spatial resolution.

For every grid-box in the model the TM defines a~~set of fluxes of a tracer in and out of~~ set of coefficients for neighbouring grid-boxes that represent the change in any tracer due to ocean circulation during a single time-step of the model (see Table 1 for an illustrative example). Using the TM in place of the model circulation, the evolution of a tracer in time is~~then~~:

$$\mathbf{c}\boldsymbol{c}^{t_{n+1}} = \mathbf{A}\mathbf{c}\mathbf{A}\boldsymbol{c}^{t_n} + \mathbf{q} \tag{1}$$

$$\boldsymbol{q}^{n} \tag{2}$$

where ~~**A**~~ **A** is the TM ~~, **c** is a~~(unitless), $\boldsymbol{c}$ is a vector representation of the gridded three-dimensional tracer field (e.g. mol ~~kg^{-1}~~kg^{-1}) with the superscript referring to the time-step ~~. **q** is a~~index. $\boldsymbol{q}$ is a vector representation of any non-circulation related sources and/or sinks for a~~tracer~~ tracer during the timestep (e.g. mol~~$kg^{-1}\ dt^{-1}$~~ kg^{-1}), for instance, due to remineralisation. Assuming steady state (where $\boldsymbol{c} = \boldsymbol{c}^{n+1} = \boldsymbol{c}^{n}$), the simplest approach to estimating remineralisation rates using Eq. (1) is to solve for ~~**q**~~ $\boldsymbol{q}$ directly, given ~~the~~ a TM and a steady state tracer~~. To achieve this practically, we use a related equation that uses the identity function (**I**) (see also Table 1 for role of **I**)~~:

$$\frac{d\mathbf{c}}{dt} = (\mathbf{A} - \mathbf{I})\mathbf{c} + \mathbf{q}$$

~~Equation (??) can then be solved for **q** by assuming $\frac{d\mathbf{c}}{dt} = 0$, i.e. as assuming steady-state:~~

$$\mathbf{q}q = -(\mathbf{A} - (\mathbf{A} - \mathbf{I})\mathbf{c} \quad (3)$$

$$\mathbf{I})\boldsymbol{c} \quad (4)$$

where **I** is the identity matrix (see Table 1 for the differences between **A** and $\mathbf{A} - \mathbf{I}$). Applying Eq. (3) with ~~a steady-state~~ an observed tracer field is the same as initialising an ocean circulation model with observed tracer concentrations and then stepping the model forward for one time step. ~~**q**~~ q will therefore reflect the exact interior source/sink terms needed in one time step to maintain the steady state tracer concentrations given the model transport rates. We refer to ~~**q**~~ q as the interior source/sink (ISS) although it is not necessarily representing a mechanistic process. q reflects the amount of remineralisation predicted over the time-step which we convert to an amount per year by multiplying by the number of timesteps within a year.

To infer particulate flux curves from estimates of the remineralisation rates, we fit a linear function to the log transformed profiles of rates vs. depth (Martin et al., 1987; Stanley et al., 2012). The gradient of the function can be related to the flux profile exponent by adding 1 (Fig. 1).

2.1 Example using a general circulation model transport matrix

As an example of the approach, we use the annual average TM derived from a 2.8° configuration of the ~~MITGCM~~ MITgcm model (available online: ~~http://www.ldeo.columbia.edu/~spk/~~http://www.ldeo.columbia.edu/~spk/) to invert a regridded annual climatogical [~~PO_4~~PO_4] field (World Ocean Atlas 2009; Garcia et al., 2010), using Eq. (3) (Fig. 2). The resulting ISS estimates at shallower depths of the

ocean interior (~~85m~~85 m) show some spatial patterns that are consistent with expectations of general export patterns, such as higher rates in the equatorial upwelling regions, and the subpolar regions of the Southern Ocean (Henson et al., 2011) (Fig. 2a). However, negative ISSs also exist, indicating a~~sink of PO_4~~ sink of PO_4, such as in regions of the subpolar Southern Ocean and Pacific equatorial upwelling. At deeper depths (~~2030m~~2030 m) the elevated values in the Southern Ocean match the shallower pattern, but overall there are fewer clear spatial features and a more random pattern of positive and negative ISSs (Fig. 2b). The existence of so many negative values gives rise to near-zero values when averaging over large spatial scales.

~~Vertical profiles of the PO_4 ISSs show a range of features~~ Linear functions were fitted to the log transformed water column profiles of estimated remineralisation rates to infer particulate flux curve exponents (Fig. 2c). ~~Several show negative values at the surface, which is expected given this will reflect uptake of $PO_4$by phytoplankton during photosynthesis. The Pacific profile at 35.17S is smooth and fitting expectations of a remineralisation curve in Fig. 1c. The profile at 4.22N however shows increasingly negative ISSs at shallower depths. This example shows that a~~ Functions were only fitted where water columns containing >3 grid-boxes with positive rates. The global mean value for b is -0.90$\pm$2.65($\pm$1 SD), close to the value found by (Martin et al., 1987) and close to values around -1.0 found when optimising ocean biogeochemical models (Kwon and Primeau, 2006). The value is smaller than the mean (b=-0.7) found in a reanalysis of globally distributed sediment trap data (Primeau, 2006) and global mean value (b=-0.639) found by (Henson et al., 2012). The value is however larger than values However, there is a wide range of values for b, including positive values, indicating an increasing flux with depth. There is also no clear pattern in the flux curves (Fig. 2. The negative ISSs and positive values for b suggest that the simple inversion of [~~PO_4~~PO_4] observations using this approach is ~~susceptable~~ susceptible to large errors that ~~will likely hinder their interpretation~~warrant further analysis to characterise and quantify potential uncertainties with this method when used with any modelled circulation.

3 ~~Methods~~

2.1 ~~Model description~~Uncertainty Analysis

2.1.1 Model description

To explore the errors when using modelled transport rates, we first derive a synthetic dataset using the Earth System model ~~'GENIE'~~ "GENIE" (Ridgwell et al., 2007a). GENIE features a 3-D ocean circulation model coupled to a 2-D energy-moisture balance model of the atmosphere and a dynamic-thermodynamic sea-ice model (Edwards and Marsh, 2005). In the configuration used here, the ocean model is non-seasonally forced and solved on a~~simplified 36x36~~ simplified 36×36 equal area horizontal grid (10~~longitude by 3- 15~~° longitude by 3–15° latitude) with 8 vertical layers. The biogeochemical model is that described in Ridgwell et al. (2007a).

Our choice of GENIE over other possible models and available transport matrices reflects a number of considerations. The configuration of GENIE used here was derived using ~~a perturbed-physics ensemble , where combinations of~~ an ensemble parameters relevant to the physical circulation were sampled from ranges to test the sensitivity of assumptions about ocean circulation and find an optimal set of parameters (Annan et al., 2005). The ensemble members are therefore different realisations of the modern ocean circulation (see Supplementary Material) The availability of this ensemble enables us to explore errors associated with uncertainty in model circulation states. The ~~annual average~~ non-seasonal circulation, coarse resolution and integration speed of GENIE also facilitate the relatively easy and fast retrieval of TMs. This is the first time that transport matrices have been constructed from an Earth system model. The relative simplicity of GENIE also keeps a focus on the methodological concept. It is worth noting that much of this could also be achieved by ~~'~~"coarse-graining~~' a~~" a TM derived from a higher resolution model, described in Khatiwala (2007), but without the availability of alternative circulation states.

2.2 ~~Diagnosing transport matrices in GENIE~~

2.1.1 Diagnosing transport matrices in GENIE

The method of Khatiwala et al. (2005) is adapted to diagnose a steady state ocean circulation simulation in GENIE. The ~~n^{th}~~ nth ocean grid-box in GENIE is dyed with 1~~mol kg^{-1}~~ mol kg^{-1} of an inert ~~'colour'~~ "colour" tracer. After the model is integrated for one time-step the resulting pattern of tracer is recovered, vectorised, and forms the ~~n^{th}~~ nth column of a~~6210x6210~~ 6210×6210 sparse matrix. This is repeated for all 6210 ocean grid-boxes in GENIE. Our method of diagnosing the TM in GENIE differs from that detailed by Khatiwala et al. (2005) in two ways. First, we do not use smoother basis vectors and instead use the simpler method of dying a single grid-box. Secondly, each grid-box is initialised only once and there is no averaging because the circulation in the 8 level version of GENIE is ~~annual average, i. e. non-seasonal.~~ non-seasonally forced. The circulation can therefore be diagnosed during a single continuous simulation. The length of the time step at which the TM is diagnosed in GENIE is 0.01 year. The TM diagnosed here includes the effects of virtual salinity fluxes applied in the ocean model to account for changes in volume (Edwards and Marsh, 2005; Ridgwell et al., 2007a). To account for this, all tracer concentrations multiplied by the TM are first normalised by the corresponding salinity field and then converted back to concentration units afterwards (Ridgwell et al., 2007a).

2.2 ~~Experiment design~~

2.1.1 Synthetic datasets

We use the biogeochemical model described in Ridgwell et al. (2007a) with the biogeochemical parameter values described in Ridgwell et al. (2007b) to produce a synthetic dataset of tracers. In this, nutrients in the surface grid-boxes are utilised by biological activity ~~in the surface ocean grid-boxes based on a nutrient and light limited scheme. A~~ limited by [PO_4] according to a Michaelis-Menton type limitation (a maximum rate of 1.96 μmol

kg^{-1} and half saturation constant of 0.22 μmol kg^{-1}) and the ambient light levels (a linear limitation term). A fixed fraction of the uptake (66 %) is exported from the surface as DOM which ~~is advected and remineralised~~ can be transported by circulation and remineralised with a time constant of $\frac{1}{0.5}$ year. The remaining fraction is exported (34 %) as particulate organic matter (POM) which remineralises instantaneously at depth according to the Martin Curve with a global b value of ~~-0.858~~ −0.858. The use of a Martin Curve keeps the discussion relevant to its use with sediment trap data and is the only difference between our model set-up and that of Ridgwell et al. (2007a, b). POM remaining in the deepest grid-box is completely remineralised to maintain a closed system, i.e. there are no sediment interactions.

2.1.2 ~~Synthetic datasets~~

[~~PO$_4$~~PO$_4$] is used as the tracer for inversion by the TM. An alternative tracer for this could be AOU (related to ~~PO$_4$~~ PO$_4$ via stoichiometric ratios), as this tracks only organic matter remineralisation (regenerated ~~PO$_4$~~PO$_4$) whilst total phosphate also includes phosphate that has been advected from the surface (preformed ~~PO$_4$~~PO$_4$). However, AOU is subject to assumptions about oxygen saturation (Ito et al., 2004; Duteil et al., 2013) and may also reflect non-biological processes (Dietze and Oschlies, 2005). To focus on errors deriving only from the method of inverting tracers, we choose to use [~~PO$_4$~~PO$_4$] over AOU. We compare our TM derived estimates of ~~PO$_4$~~ PO$_4$ remineralisation with the ~~total remineralisation of phosphate~~actual model remineralisation of PO$_4$ in each grid-box as diagnosed within the experiment run as mol~~PO$_4$ kg^{-1} year^{-1} and is converted to dt^{-1} by dividing by the number of timesteps per year (96; =0.01 year^{-1})~~ PO$_4$ kg^{-1} year^{-1}. The [~~PO$_4$~~PO$_4$] field is the annual average taken from the last year of a~~10000 year~~ 10 000 year spin-up. A corresponding TM is diagnosed at the end of the ~~10000 year~~ 10 000 year run. This synthetic dataset is referred to as SYN~~(Table **??**). A~~. A second synthetic dataset (SYN-NODOM) is also produced in the same way as the SYN dataset except no DOM is produced to explore the effect of DOM when inferring flux curves from remineralisation rates.

2.1.2 Experiments

We design a number of experiments to explore the sensitivity of the approach to various sources of error (experiment names are indicated in brackets~~and also described in Table ??~~):

1. (TWIN) We first use the TM corresponding to the synthetic dataset (SYN) to estimate remineralisation rates from the corresponding [~~PO_4~~PO_4] field as a proof of concept of the method (a twin-test)~~.~~, i.e. to test that the modelled remineralisation rates can be recovered by applying the TM to the modelled [PO_4] field.

2. (ERR-OBS) The effect of errors from the tracer observations themselves is simulated by calculating 100 random perturbations to the synthetic ~~PO_4~~ PO_4 concentrations (SYN) within one ~~standard deviation~~SE. For each grid-box, the mean is taken as the synthetic ~~PO_4~~ PO_4 concentration (SYN), and one ~~standard deviation from the standard deviation of WOA~~ SE from the SE of World Ocean Atlas (WOA) [~~PO_4~~PO_4] observations regridded to the GENIE grid (Garcia et al., 2010).

3. (ERR-CIRC) To explore the effect of circulation uncertainty, we diagnose 54 individual TMs from an existing perturbed physics ensemble (Annan et al., 2005). The ensemble is the result of tuning circulation parameters to fit modern temperature and salinity fields using an ensemble Kalman filter. Each ensemble member is spun-up for ~~10000 years~~ 10 000 years after which the TM is diagnosed and used to invert the synthetic [~~PO_4~~PO_4] field (SYN). The circulation parameters in Ridgwell et al. (2007a, b) are an average of the ensemble parameters, such that the 54 TMs offer a range of different ocean circulation states. Details of the ensemble parameters and comparisons against the standard configuration can be found in the ~~supplementary material~~Supplement.

4. (ERR-DOM) We explore the effect of DOM when inferring particulate flux curves from remineralisation rates. As a comparison to the synthetic dataset, we run an identical experiment but with no DOM created (SYN-NODOM), i.e. all ~~PO_4~~ PO_4 is exported as particulate organic matter.

3 ~~The transport matrix inversion method~~Uncertainty Analysis Results

3.1 Assessment of the transport ~~natrix~~ matrix inversion method

We use the output from GENIE as a synthetic dataset from which to assess the transport matrix inversion method and identify the sources and nature of the errors involved. Figure~~3a and 3~~ 3a and b show the [~~PO_4~~PO_4] field in GENIE at two depths, directly below the surface (~~290m~~290 m) and in the deep ocean (~~2106m~~2106 m), with the corresponding annual average input of ~~PO_4~~ PO_4 from the continual remineralisation of sinking particles and dissolved organic matter at the same depths (Fig. 3c and ~~3~~d). The higher remineralisation values calculated for single grid-boxes occur where the remaining particulate flux is remineralised at the seafloor to maintain a closed system, i.e. to ensure there are no losses to sediments (Fig. 3d). We also show the inventory of phosphorus in DOM integrated over the ocean interior below ~~175m~~ 175 m (Fig. 3e). DOM has a visually similar pattern to shallow ~~PO_4~~ PO_4 remineralisation, because they are both linked by export production. The close resemblance and magnitude of the DOM at shallow depths may have implications for using remineralisation rates to infer remineralisation fluxes which will be discussed in ~~section~~ Sect. 4.2. Finally, we note a correspondence between areas in the Southern Ocean with a large magnitude of remineralisation at shallow depths and locations where convection occurs in the model (Fig. 3f). This is consistent with high productivity driven by nutrients delivered to the surface via strong vertical mixing.

3.1.1 ~~Twin-test~~

To demonstrate and test the method described in ~~section~~ Sect. 2, we first invert the model generated synthetic [~~PO_4~~PO_4] field using the corresponding TM as per Eq. (3) (Fig. 4a). The interior source/sink term (ISS) calculated by inverting the synthetic [~~PO_4~~PO_4] field is consistent with the model calculated remineralisation with minor deviations from the ~~1:1~~ 1 : 1 ratio line (Fig. 4a). This demonstrates the success of the approach as the errors in the synthetic tracer field and circulation scheme are effectively reduced to near-zero in

this example. The errors between estimated and modelled remineralisation rates cluster around zero with a median proportion of error of ~~1.1x10^{-3}~~ 6.3×10^{-5} (Fig. 4b). ~~Some larger errors , i.e. the outliers to the 1:1 line in Fig. 4a, occur in distinct regions such as in the shallow sub-tropics (Fig. 4e) and the deep equatorial Atlantic (Fig. 4f). These errors likely represent either,~~ Minor errors likely represent small differences in the circulation at individual time-steps that have been sampled by our method of sequentially dying grid-boxes during a~~single run, or are a result of the model circulation not being in strict steady state~~ single run. Overall however the TM inversion of the synthetic [~~PO_4~~PO_4] estimates the ~~PO_4~~ PO_4 remineralisation rates very well (Fig.~~4e and 4f c. f. Fig.~~ 4c and 4d cf. Fig. 3c and 3d) with minor errors. This demonstrates that, in theory at least, modelled circulation rates in the form of a transport matrix can be used to successfully estimate remineralisation rates from a tracer field.

3.2 Sensitivity of inversions to sources of errors

Although remineralisation rates can be estimated by applying transport rates to a tracer field as shown above, there are several assumptions that will introduce error when this is applied to observations. In the following sections, we detail the results of experiments designed to explore these sources of error.

3.2.1 Error from observations

Error related to the 1° World Ocean Atlas annual mean climatology (Garcia et al., 2010) will introduce some uncertainty in the TM inversion due to measurement errors and biases in the climatology itself~~as well as re-gridding the observations onto a model grid such as GENIE or MITGCM~~. As a measure of how sensitive the TM inversion method is to these errors, we regrid the ~~standard deviation~~ SE of annual [~~PO_4~~PO_4] observations onto the GENIE grid (Fig. 5). ~~The standard deviations~~ We do not consider any additional uncertainty here that may arise through the re-gridding process, i.e. Kriest et al. (2002). The SEs in each grid-box are used to produce an illustrative estimate of the uncertainty inherent in

the observations. The ~~standard deviations~~ SEs are highest in the coastal regions and high latitudes, and at shallower depths (Fig.~~5a c. f. Fig. 5~~ 5a cf. b). We note that errors in the observations may be spatially correlated which will warrant consideration in future work.

The ~~standard deviations~~ SEs are used to produce 100 versions of the synthetic [~~PO_4~~PO_4] field that have been perturbed within the observation uncertainty which are then inverted using the TM. The resulting ~~standard deviation of the PO_4 ISSs~~variability in the PO_4 ISSs, as characterised by the SD, are relatively large compared to the ISS values themselves, around ~~1-3~~ 1–3 orders of magnitude larger than the ISS values ~~.~~ (see also Fig. 8). There are positive linear trends between the ~~standard deviation of~~ SD of the 100 perturbed observations in each grid-box and the ~~standard deviation~~ SD of the 100 corresponding ISS estimates in each grid box (Fig. 5c). Grid-boxes with higher uncertainty in the observation results in greater uncertainty in the ISS estimates. However, two ~~distributions~~ clusters can be broadly defined in Fig. 5c both with separate linear trends that correspond well with the size of the ~~'flux out'~~ "flux out" term of the TM (see Table 1). The colour scale gives an indication of the relative size of the flux out for each grid-box due to circulation. Where the central grid-box coefficient is ~~smaller in the TM, leading to correspondingly largervalue when used in Eq. (3) (e.g. $1 - \mathbf{A}$)~~larger, the uncertainty in ISS arising from the uncertainty in the observations is much more sensitive. This suggests that the ISS uncertainty is ~~a~~ partly a function of the ~~way the TMis constructed.~~circulation diagnosed in the TM, i.e. if the observation uncertainty were fixed to a constant across all grid-boxes, ISSs in some grid-boxes will have greater uncertainty than others due to this effect. The flux out term is largest in areas in our TM where convection occurs, i.e. the Southern Ocean and North Atlantic (Fig. 3f), because this is where the largest transport fluxes are in the model ~~.~~ (Fig. 5d).

3.2.2 Error from circulation estimates

Another potential source of error when inverting nutrient observations arises from the use of a modelled circulation field that will inevitably have a somewhat poorly quantified relationship to the circulation of the real ocean. Using ~~a perturbed physics~~ TMs representing

plausable but different realisations of the modern ocean circulation from an ensemble to invert our synthetic dataset, we can explore the effect of errors arising from uncertainties in circulation rates only. ~~Fig. 6a~~Figure 6a shows the mean and 1 ~~standard deviation~~ SD of the ISS estimates generated when inverting the synthetic [~~PO_4~~PO_4] field with all 54 ensemble TMs. The values furthest from the ~~1:1~~ 1 : 1 ratio line and those with the largest error bars are located in regions where convection occurs in the model (Fig.~~6a~~ 6a and 6c). The strength of overturning varies within the ensemble (see ~~supplementary material~~Supplement) suggesting that this structural uncertainty in the model is a likely cause for the wide range of remineralisation estimates. An additional issue is that unlike most grid-boxes in our TM, where the spread of a tracer over one timestep is limited to neighbouring grid-boxes, convection increases the number of grid-box connections in the vertical. This could have the effect of increasing the range of remineralisation estimates because there are more grid-boxes. ~~Fig.~~ Figure 6b shows the same as Fig.~~6a~~ 6a but with the convection-related values removed. Even in areas where there is no convection in the model, the range of ISS estimates from circulation uncertainty is larger relative to the range of remineralisation values. The range of errors arising from using different circulations are also larger at shallower depths compared to deeper depths in the water column (Fig. 6c and 6d).

To understand why different circulation estimates can have a large impact of ISSs, we explore the size of the ~~PO_4~~ PO_4 remineralisation flux in a grid box relative to the size of ~~PO_4~~ PO_4 flux from the modelled circulation. To illustrate this, we compare the steady state circulation flux of ~~PO_4 into a~~PO_4 into a grid-box with the remineralisation flux of ~~PO_4~~ PO_4 into each grid-box from the synthetic run (the sum of these at steady state will equal the flux of PO_4 out of the box). Across the whole model ocean interior, the mean proportion of remineralisation flux to the total flux into each grid box is ~~0.001±0.015 (±1 standard deviation~~0.005 ± 0.025 (± 1 SD). The proportion is generally 2 magnitudes of order higher at shallower depths (~~290m~~290 m) than at depth (~~2106m~~2106 m) (Fig.~~7a c. f. Fig. 7~~ 7a cf. b), reflecting the decrease in remineralisation fluxes with depth whilst circulation fluxes ~~are generally the same magnitude~~ vary much less in magnitude in GENIE (Fig. 7c and 7d).

Even relatively small errors in the circulation ~~flux~~ fluxes are therefore likely to dominate over the remineralisation fluxes leading to large errors when using modelled circulation rates.

3.2.3 Error comparison

To compare the magnitude of the various possible errors, we show the global mean synthetic ~~PO_4~~ PO_4 remineralisation profile with the global mean and median ~~standard deviations~~ SDs of the ISSs calculated from the ERR-OBS and ERR-CIRC experiments (Fig. 8). We use both the mean and median ~~standard deviation~~ SD in this figure because the mean ~~standard deviation~~ SD of the ERR-CIRC experiments are skewed by the large variability in high latitude regions (Fig. 6a). Both sources of error are larger at shallower depth and mostly decrease in magnitude with depth although the mean circulation uncertainty increases below ~~2000m~~2000 m. The magnitude of median uncertainty from the observations is much larger than from our circulation estimates although the two are similar magnitudes when the mean ~~standard deviation is usedto calculate profiles~~SD is used.

Despite similar magnitudes of uncertainty arising from both potential errors in the observations and from the model circulation field, the nature of the uncertainty is different. Uncertainty from the observations is higher in regions where observations are more uncertain, e.g. coastal areas in Fig.~~5a and 5~~ 5a and b, and in regions of the model where convection occurs (Fig. 5c). In contrast, the uncertainty arising from the model circulation field used will be systematic and dependent on where the model circulation is most different to the real ocean, e.g. Fig.~~6. The~~ 6. Although the patterns in the surface ~~PO_4~~ PO_4 ISSs from the ~~MITGCM~~ MITgcm inversion are systematic ~~which may suggest that errors are predominantly related to the ocean model (Fig.~~ (patches of positive and negative ISSs in the Southern Ocean: Fig 2a)~~although this is less the case for the deeper ocean (Fig. 2b).~~ , it is difficult to tell whether this reflects a systematic difference between observed and modelled circulation rates, or a caveat associated with convection in the model and larger circulation fluxes in these areas. The relative smoothness of the ISS estimates may reflect the use of the climatology which has already been smoothed (Garcia et al., 2010).

4 Inferring flux curves from remineralisation rates

3.1 Vertical profiles and dissolved organic matter

In the previous section, we have shown that a simple approach to estimating remineralisation rates using modelled transport ratesis sensitive to errors. Taking the next step, in the case that remineralisation rates could be estimated with some reliability, we explore the sensitivity of inferring flux curves by vertically integrating remineralisation rates in the presence of DOM. We infer flux curves using remineralisation rates from the synthetic dataset (SYN) and a second run where no DOM is exported (SYN-NODOM). To infer a power law curve, a linear trend in fitted to the log transformed remineralisation rates following previous studies . The gradient of the linear trend gives the value of the exponent for the remineralisation curve, which is converted to a flux curve by adding 1 (; See also Fig. 1).

The exponents from power-law curves, fitted to vertical PO_4 remineralisation profiles, when PO_4 is only exported as particulate organic matter, are all close to -1.9 (Fig. 10a). This corresponds to a flux curve exponent of -0.9, in good correspondence with -0.858 used for the run. The presence of remineralisation from DOM (see Fig. 3e) lowers the value of the fitted exponent reflecting a shallower Martin Curve (Fig. 10b). In our experiments, the remineralisation of DOM lowers the fitted exponent by as much as 0.6. This occurs because the remineralisation of DOM inflates the remineralisation rate in the shallower grid-boxes relative to those in the water column below. The fitted flux curve is shallower to reflect more remineralisation occurring at shallower depths. The DOM bias in GENIE occurs predominantly in the high latitudes where DOM is efficiently advected into the ocean interior. The range of exponents purely from this bias is of a similar magnitude and spatial distribution to the Martin Curve exponents found in .

4 Discussion~~and way forward~~

We have presented a straightforward method of using a steady state model circulation, as represented by a transport matrix, to estimate organic matter remineralisation rates from a tracer climatology. Our main goal is to explore the feasibility of using this method to infer spatially explicit organic matter flux curves aiding additional understanding of the biological pump in the modern ocean. Our results show that this method is associated with a number of significant sources of error that give rise to the spatial patterns and negative values seen in an example inversion using a circulation field from a ~~high~~ coarse resolution ocean model (Fig. 2). In the following sections we discuss potential directions for estimating remineralisation rates from tracer data using model circulation and additional considerations needed when using these to infer particle flux curves.

The sensitivity to errors in the observations is a result of the way that the transport matrix (TM) is constructed. A change in a tracer due to circulation in a model time-step is relatively localised due to the finite speed of advection and diffusion in the model (Khatiwala et al., 2005). Therefore, the ISS estimates are sensitive to the resulting large coefficient in the central grid-box (see Table 1). This will be a feature of all TMs constructed using the method of Khatiwala et al. (2005) regardless of ~~resolution. Previous methods have relied on relating multiple tracers together such that the model transport terms cancel out e. g. and is a method which could be applied using the TM. The sensitivity to uncertainty in the tracer observations however, may pose a problem, especially if observational errors are different between tracers.~~

the resolution or model used. Our results also illustrate the sensitivity of remineralisation estimates to differences between the model transport rates and actual transport rates in the ocean. Remineralisation fluxes of ~~PO_4~~ PO_4 in the synthetic tracer experiments are orders of magnitude smaller than fluxes of ~~PO_4~~ PO_4 from circulation. Model transport rates would therefore need to attain a high level of accuracy to minimise the effect of error on the solutions (Anderson and Sarmiento, 1994; Sarmiento et al., 2002). Even a data assimilated model, such as produced by the ECCO Consortium (~~"~~"Estimating the Circulation and

Climate of the Ocean~~';~~ ~~"~~; Stammer et al., 2004), designed to be a dynamically consistent estimate of ocean circulation over recent decades may still lead to large diagnosed flux errors. An additional consideration may also be the representation of a steady state in the TM, either because a model is not spun up fully or because there is seasonality.

4.1 Are there constraints on the circulation uncertainty?

The flipside of the magnitude and nature of the circulation control on the diagnosed remineralisation rates is that tracers with a steady-state constraint, where it is expected that there should be no significant sources or sinks at depth, could be used to estimate the magnitude of the circulation-based error. As an example, we show an ISS field generated when inverting the salinity field from our synthetic dataset with the synthetic transport matrix (Fig.~~9a and 9~~ 9a and b). Salinity ISS are randomly distributed around zero, consistent with the concept that salinity is not significantly increasing or decreasing in the ocean interior. In comparison, applying a different transport matrix, arbitrarily chosen from the ~~perturbed physics ensemble~~ ensemble of alternative modern circulations, results in distinct spatial patterns in the ISSs (Fig. 9c and ~~9~~d). Comparing the errors from the inversion of the synthetic [~~PO$_4$~~PO$_4$] field using the same TM shows that the two ~~are visibly similar~~ have some visible similarities (Fig. 9e and f). For example, there are correspondences in the deep South Atlantic (Fig. 9~~e and 9f).~~ d and e) and the subtropical regions of the Pacific at 290m (Fig. 9c and e). We do not expect an exact correspondence but the visual similarities support the idea that they are related via errors in the model circulation. This suggests that conservative tracers, i.e. tracers that do not have sources or sinks in the ocean interior~~could constrain~~, could provide a constraint on the magnitude of error. For example, considering Eq. (3) but focussing on an individual grid-box, the ISS (**q**~~$_{i=1}$~~$q_{i=1}$) is a function of the TM coefficients (M_i) and the tracer concentrations (C_i) as per the example in Table~~1:~~ 1:

$$\mathbf{q}q_{i=1} = \sum_{i=1}^{N} M_i C_i \tag{5}$$

(6)

Redfining the modelled circulation terms to reflect that the modelled circulation is a function of a ~~'true'~~ "true" circulation term and an error term ($M_i = F_i + \epsilon_i$) and substituting into ~~5~~ Eq. (5) and expanding:

$$\mathbf{q}\boldsymbol{q}_{i=1} = \sum_{i=1}^{N} F_i C_i + \sum_{i=1}^{N} \epsilon_i C_i \tag{7}$$

(8)

For a conservative tracer at steady state, it is expected that $\sum_{i=1}^{N} F_i C_i = 0$. A significant departure from zero in $\mathbf{q}_{i=1}$ ~~$\boldsymbol{q}_{i=1}$~~ is likely to result from the error terms. This may provide a way forward to constrain the ISSs produced by the TM method described here. Such a method would be conceptually similar to the ~~mixing model approaches that use steady state constraints~~ TMI method (Gebbie and Huybers, 2010). There are however, a limited number of tracers available (e.g. temperature, salinity, δ^{18}O, Δ^{14}C, CFCs) that could realistically be used to constrain model circulation errors. Of these tracers, CFCs are not yet present in the deep ocean and so are not in steady state. In our TM, there are typically 15 grid-box connections (6 neighbouring grid-boxes plus extra connections due to the Gent-McWilliams parametersation) used for each calculation which would lead to an underdetermined solution, i.e. where the unknowns outnumber the constraints. It would be interesting to see if a simplified TM with fewer coefficients, such as matching the method of Gebbie and Huybers (2010) by adopting a 7-point stencil (6 neighbouring grid-boxes), could use this approach. Even so, with a 7-point stencil, the solution may still be underdetermined.

~~We have also shown that the remineralisation of dissolved organic matter can potentially bias the estimation of flux curves from remineralisation rate profiles. In particular, this bias,~~

~~at least in our model, causes spatial variability in flux curves that is similar in pattern and magnitude to patterns of particulate organic carbon fluxes found in global sediment trap studies .~~

4.2 Inferring flux curves from remineralisation rates

In the previous sections, we have shown that a simple approach to estimating remineralisation rates using modelled transport rates is sensitive to different sources of errors. Taking the next step, in the case that remineralisation rates could be estimated with some reliability, we explore the sensitivity of inferring flux curves by vertically integrating remineralisation rates in the presence of DOM. The remineralisation of DOM can occur away from where it was exported, affecting the assumption that the remineralisation rates reflect only vertical processes. To explore this, we infer flux curves using remineralisation rates from the synthetic dataset (SYN) and a second run where no DOM is created (SYN-NODOM). To infer a power law curve, a linear trend in fitted to the log transformed remineralisation rates following previous studies (Berelson, 2001; Lam et al., 2011; Stanley et al., 2012). The gradient of the linear trend gives the value of the exponent for the remineralisation curve, which is converted to a flux curve by adding 1 (Martin et al., 1987; Stanley et al., 2012; see also Fig. 1).

The exponents from power-law curves, fitted to vertical PO_4 remineralisation profiles, when PO_4 is only exported as particulate organic matter, are all close to -1.9 (Fig. 10a). This corresponds to a flux curve exponent of -0.9, in good correspondence with -0.858 used for the run. The presence of remineralisation from DOM (see Fig. 3e) lowers the value of the fitted exponent reflecting a shallower Martin Curve (Fig. 10b). In our experiments, the remineralisation of DOM lowers the fitted exponent by as much as 0.6. This occurs because the remineralisation of DOM inflates the remineralisation rate in the shallower grid-boxes relative to those in the water column below. In a few grid-boxes in the North Atlantic the estimate of the flux curve exponent increases. This has a strong correspondence with the deepest convection (Fig. 3f) where DOM is transported deeper into the water column before being remineralised. This highlights that an additional source of remineralisation not

restricted to vertical processes, such as the remineralisation of DOM, can alter the flux curve in an unpredictable way. The DOM bias in GENIE occurs predominantly in the high latitudes where DOM is efficiently advected into the ocean interior. The range of exponents purely from this bias is of a similar magnitude and spatial distribution to the Martin Curve exponents found in Henson et al. (2012).

4.3 The way forward

Any method of ~~estimating~~ inferring particulate organic matter flux curves from estimated ~~organic matter~~ remineralisation rates, whether using model transport rates or using ~~AOUR,~~ observations, e.g. Stanley et al. (2012), will therefore need to take the remineralisation of DOM (as well as other processes not constrained to the vertical water column such as denitrification) into account, particularly in regions where DOM is advected to deeper depths (Hansell et al., 2009). ~~This~~ Ultimately, this additional source of uncertainty ~~could be handled using other modelling approaches such as optimisation~~ when inferring flux curves combined with the uncertainties associated with estimating remineralisation rates suggests this is a difficult task. An alternative approach, that explicitly includes the effects of DOM remineralisation is the optimisation of ocean biogeochemical models. In this approach, a biogeochemical model is set-up and optimal values of the parameters found, such as the depth of remineralisation, ~~the production of DOM and~~ export production and the rate of DOM remineralisation, ~~found~~ that result in the best fit between modelled and observed nutrient fields, e.g. ~~.~~ , Bacastow and Maier-Reimer (1991); Schlitzer et al. (2002); Kwon and Primeau (2006); Kriest et al. (2012); Yao and Schlitzer (2013); Teng et al. (2014). For example, remineralisation depths could be varied in space and a solution found that best fits tracer observations. A first step towards this has been taken by Yao and Schlitzer (2013). Such an approach allows additional constraints such as export production magnitude to be taken into account as well as providing further evaluation on circulation models via biogeochemical tracers (Najjar et al. , 2007). Transport matrices are a useful tool in this approach to help ~~avoid~~ reduce lengthy multi-thousand year integration times for model fields to reach equilibrium as well as providing alternative methods to

efficiently reach steady state solutions (Kwon and Primeau, 2006). ~~Given the uncertainties we have highlighted, a range of approaches may be needed to fully explore and quantify remineralisation rates and flux curves~~Ultimately, the approach of optimising biogeochemical models is complimentary to the approach described in this paper as they both rely on the combination between observations and models but in different ways, which could help facilitate a better understanding of biogeochemistry as well as of the models used to study it.

5 Conclusions

~~Spatial patterns in particulate fluxes suggest particular mechanisms that control the distribution of remineralisation in the ocean interior.~~ Profiles of remineralisation rates derived from ocean tracers offer a potential method to estimate high resolution fields of flux curves that could supplement existing global sediment trap studies. The use of model transport rates offers one way of estimating remineralisation rates that could avoid the spatial averaging issues of combing AOU with age tracers. ~~Through the use of a simple method using the Transport Matrix, we have shown that a high level of accuracy would be needed as remineralisation rates are an order of magnitude smaller than circulation fluxes. Aside from the errors~~ Using the transport rates in the form of a transport matrix is a first step towards this but the simple application to a tracer such as [PO_4], to estimate steady state remineralisation rates, is subject to potentially large uncertainties related to both uncertainties in the observations ~~themselves, which for the method presented were also large, the uncertainty when using modelled circulation rates is an important issue. To get information about particle fluxes, the remineralisation rates also need to be integrated vertically. This process is also associated with uncertainty due to~~ and the modelled transport rates. There are potential methods to constrain the uncertainty in the modelled transport rates which are currently limited by the number of tracers available. We also highlight that there significant uncertainties when integrating remineralisation rates vertically, necessary to estimate particle flux curves, associated with processes such as

the remineralisation of ~~DOM. Both these sources of uncertainty are key issues to be considered for future approaches in quantifying the remineralisation of organic matter in the ocean interior~~dissolved organic matter. This last uncertainty has implications for deriving flux curves from data-based estimates of remineralisation rates as well as model-based ones.

The spatial variability in POC fluxes observed in the modern ocean has important implications for our understanding of how the biological pump may have changed in the past and in the future. New approaches to estimating POC fluxes will help provide estimates in regions, such as the Southern Ocean, that are currently undersampled by sediment traps and key to testing existing mechanistic hypotheses. Exploring the spatial variability of POC fluxes in ocean biogeochemical models by finding a set of POC flux profiles that best fits observed tracers will help approach the uncertainties highlighted in this paper but also provide a quantitative analysis of the significance of spatially varying POC fluxes.

The Supplement related to this article is available online at doi:10.5194/bgd-0-1-2015-supplement.

Acknowledgements. This work was conducted as part of a project studentship (~~JDW~~J. D. Wilson) associated with the UK Ocean Acidification Research Programme (UKOARP) grant NE/H017240/1 to ~~AR and SB.JDW and AR~~ A. Ridgwell and S. Barker. J. D. Wilson and A. Ridgwell acknowledge support via EU grant ERC-2013-CoG-617313. ~~AR acknowledges~~ A. Ridgwell also aacknowledges support from a ~~Royal Society University Research Fellowship~~Leverhulme award RPG-2013-106. We thank Samar Khatiwala for making code and matrices available online and Julia Hargreaves for providing the ensemble data.

References

Anderson, L. A. and Sarmiento, J. L.: Redfield ratios of remineralization determined by nutrient data analysis, Global Biogeochem. Cy., 8, 65–80, doi:10.1029/93GB03318, 1994.

Annan, J., Hargreaves, J., Edwards, N., and Marsh, R.: Parameter estimation in an intermediate complexity earth system model using an ensemble Kalman filter, Ocean Model., 8, 135–154, doi:10.1016/j.ocemod.2003.12.004, 2005.

Archer, D. and Maier-Reimer, E.: Effect of deep-sea sedimentary calcite preservation on atmospheric CO_2 concentration, Nature, 367, 260–263, doi:10.1038/367260a0, 1994.

Armstrong, R. A., Lee, C., Hedges, J. I., Honjo, S., and Wakeham, S. G.: A new, mechanistic model for organic carbon fluxes in the ocean based on the quantitative association of POC with ballast minerals, Deep-Sea Res. Pt. II, 49, 219–236, 2002.

Bacastow, R., and Maier-Reimer, E.,: Dissolved organic carbon in modelling new production, Global Biogeochemical Cycles, 5, 71–85, 1991.

Berelson, W.: The flux of particulate organic carbon into the ocean interior: a comparison of four U.S. JGOFS regoinal studies, Oceanography, 14, 59–67, 2001.

Broecker, W. S., Peacock, S. L., Walker, S., Weiss, R., Fahrbach, E., Schroeder, M., Mikolajewicz, U., Heinze, C., Key, R., Peng, T.-H., and Rubin, S.: How much deep water is formed in the Southern Ocean?, J. Geophys. Res.-Oceans, 103, 15833–15843, doi:10.1029/98JC00248, 1998.

Buesseler, K.O., Antia, A. N., Chen, M., Fowler, S.W., Gardner, W.D., Gustafsson, O., Harada, K., Michaels, A.F., Rutgers v. d. Loeff, M., Sarin, M., Steinberg, D.K., and Trull, T.: An assessment of the use of sediment traps for estimating upper ocean particle fluxes, Journal of Marine Research, 3, 345–416, 2007.

~~The range of observed Martin Curves and associated remineralisation rate profiles (a) The mean (b=-0.639) and global range (b=-1.18 to -0.24) of Martin Curves found by calculated for a unit flux and export depth (z_0) via $F_z = 1 * \frac{z}{z_0}^{-b}$ (b) The first derivativee of each flux curve in panel a, equivalent to a vertical profile of organic matter remineralisation calculated as $\frac{dF_z}{dz} = \frac{-b}{z_0} * \frac{z}{z_0}^{-(b-1)}$.~~

Deutsch, C., Sarmiento, J. L., Sigman, D. M., Gruber, N., and Dunne, J. P.: Spatial coupling of nitrogen inputs and losses in the ocean, Nature, 445, 163–167, doi:10.1038/nature05392, 2007.

~~Example of using a GCM transport matrix to estimate PO_4 remineralisation rates. (a) The estimated PO_4 remineralisation rates generated using the MIT GCM transport matrix at 85m and (b) 2030m. (c) Vertical profiles of PO_4 remineralisation rates estimated using transport rates from an MITGCM transport matrix (equivalent to Fig. 1b) are shown from latitudes corresponding to equivalent regions in the Pacific at 223E.~~

Dietze, H. and Oschlies, A.: Modeling abiotic production of apparent oxygen utilisation in the oligotrophic subtropical North Atlantic, Ocean Dynam., 55, 28–33, 2005.

The synthetic tracer dataset used for transport matrix inversions. (a) PO_4(μmol kg^{-1}) at 290m and (b) 2106m. (c) the total annual remineralisation flux of PO_4 (nmol kg^{-1} dt^{-1}) at 290m and (d) 2106m. (e) the water column integrated inventory of phosphorus in dissolved organic matter in the ocean interior (mol P). (f) a cost function for convection occurring in a water column in one model year (unitless). Higher values indicate stronger convection in the model.

Duteil, O., Koeve, W., Oschlies, A., Bianchi, D., Galbraith, E., Kriest, I., and Matear, R.: A novel estimate of ocean oxygen utilisation points to a reduced rate of respiration in the ocean interior, Biogeosciences, 10, 7723–7738, doi:10.5194/bg-10-7723-2013, 2013.

Results from inverting the synthetic dataset with its corresponding transport matrix. (a) The interior source/sink estimate for PO_4 when inverting the synthetic PO_4field with the corresponding transport matrix versus the synthetic PO_4 remineralisation with a 1:1 ratio line, (b) the distribution of errors for the PO_4 interior source/sink estimates (50 bins sized 0.15x10^{-5}). (c) the interior source/sink estimate for PO_4 at 290m and (d) 2106m. (e) Difference between inverse interior source/sink estimates and the synthetic remineralisation field at 290m and (f) 2106m.

Edwards, N. and Marsh, R.: Uncertainties due to transport-parameter sensitivity in an efficient 3-D ocean-climate model, Clim. Dynam., 24, 415–433, 2005.

Assessment of the errors arising from the uncertainty in PO_4observations. (a) the standard deviation of $PO_4$from the World Ocean Atlas 2009 1climatology regridded to the GENIE grid at 290m and (b) 2106m. (c) Standard deviation of all PO_4 interior source/sink estimates when the synthetic PO_4field is randomly perturbed within a normal distribution given by the standard deviation of observations. The two distributions are distinguished by the value of the TM coefficient in the same grid-box shown by the colour bar. A linear regression trend line fitted to data where the coefficient is $>$0.8 (dotted line) gives a slope of 0.03 (R^2=0.71). When fitted to data $<$0.8 (dashed line), the slope is 0.63 (R^2=0.84).

Feely, R., Sabine, C., Schlitzer, R., Bullister, J., Mecking, S., and Greely, D.: Oxygen utilization and organic carbon remineralization in the upper water column of the Pacific Ocean, J. Oceanogr., 60, 45–52, 2004.

Assessment of error arising from using circulation estimates. a) Comparison of ISS estimates for each grid-box from the 54 ensemble members against the synthetic dataset remineralisation. Error bars are 1 standard deviation around the mean. Red values indicate regions with convection. b) As panel a but with the red values removed. Note the difference in scale. c) The standard deviation of PO_4 ISS errors (Model - ISS) in μmol kg^{-1} dt^{-1} for 290m. Values are shown on a log scale. d) As panel c but at 2106m.

Garcia, H., Locarnini, R., Boyer, T., Antonov, J., Zweng, M., Baranova, O., and Johnson, D.: World Ocean Atlas 2009, Volume 4: Nutrients (phosphate, nitrate, silicate), in: NOAA Atlas NESDIS 71, edited by: Levitus, S., U.S. Government Printing Office, Washington, DC, 398 pp., 2010.

~~Comparison of inputs of PO_4 from remineralisation and circulation at steady-state. (a) PO_4 remineralisation as a proportion of the total PO_4 flux into each grid-box calculated using the synthetic tracer field at 290m and b) 2106m. c) the flux of PO_4 into each grid-box from circulation only (μmol kg^{-1} dt^{-1}) from the synthetic tracer fields at 290m and d) 2106m.~~

Gebbie, G. and Huybers, P.: Total matrix intercomparison: a method for determining the geometry of water-mass pathways, J. Phys. Oceanogr., 40, 1710–1728, doi:10.1175/2010JPO4272.1, 2010.

~~Comparison of error magnitudes when estimating remineralisation rates. The global mean PO_4 remineralisation profile from the synthetic dataset is shown with the plus and minus the mean and median standard deviations from the ERR-OBS and ERR-CIRC experiments.~~

Gebbie, G. and Huybers, P.: The Mean Age of Ocean Waters Inferred from Radiocarbon Observations: Sensitivity to Surface Sources and Accounting for Mixing Histories, J. Phys. Oceanogr., 42, 291–305, doi:10.1175/JPO-D-11-043.1, 2012.

~~Assessment of the uncertainty associated with dissolved organic matter when inferring flux profiles. Value of the exponent when fitting a power law to the water column remineralisation rates from a) a model with remineralisation from only sinking particulate and b) a model with particulate and dissolved organic matter. A value of -0.858 for the Martin Curve was used in both models. All curves were fitted with an $R2 > 0.9$. The exponent for the remineralisation curve is equivalent to -0.858 ± 1. More negative values indicate a Martin Curve that predicts shallower remineralisation in the water column. Hatched areas indicate where the water column contained too few boxes to fit a remineralisation curve ($n<3$).~~

Hansell, D., Carlson, C., Repeta, D., and Schlitzer, R.: Dissolved organic matter in the ocean: a controversy stimulates new insights, Oceanography, 22, 202–211, 2009.

~~Inversion of salinity as a possible constraint on the uncertainty from using a modelled circulation. (a) Inversion of the salinity field from the synthetic dataset using the corresponding transport matrix at 290m (PSU dt^{-1}) and at (b) 2106m. (c) Inversion of the salinity field using a alternative transport matrix from the perturbed-physics ensemble (PSU dt^{-1}) at 290m and (d) 2106m. (e) The error of the synthetic PO_4 ISS (μmol kg^{-1} dt^{-1}) (ISS-synthetic) using the same transport matrix in panels c and d at 290m and f) 2106m.~~

Henson, S., Sanders, R., and Madsen, E.: Global patterns in efficiency of particulate organic carbon export and transfer to the deep ocean, Global Biogeochem. Cy., 26, GB1028, doi:10.1029/2011GB004099, 2012.

Henson, S. A., Sanders, R., Madsen, E., Morris, P. J., Le Moigne, F., and Quartly, G. D.: A reduced estimate of the strength of the ocean's biological carbon pump, Geophys. Res. Lett., 38, L04606, doi:10.1029/2011GL046735, 2011.

Honjo, S., Manganini, S. J., Krishfield, R. A., and Francois, R.: Particulate organic carbon fluxes to the ocean interior and factors controlling the biological pump: a synthesis of global sediment trap programs since 1983, Prog. Oceanogr., 76, 217–285, doi:10.1016/j.pocean.2007.11.003, 2008.

Honjo, S., Eglinton, T., Taylor, C., Ulmer, K., Sievert, S., Bracher, A., German, C., Edgcomb, V., Francois, R., Iglesias-Rodriguez, M., Van Mooy, B., and Repeta, D.: Understanding the role of the biological pump in the global carbon cycle: an imperative for ocean science, Oceanography, 27, 10–16, 2014.

Ito, T., Follows, M. J., and Boyle, E. A.: Is AOU a good measure of respiration in the oceans?, Geophys. Res. Lett., 31, L17305, doi:10.1029/2004GL020900, 2004.

Jenkins, W. J.: Oxygen utilization rates in North Atlantic subtropical gyre and primary production in oligotrophic systems, Nature, 300, 246–248, doi:10.1038/300246a0, 1982.

Jin, X., Gruber, N., Dunne, J. P., Sarmiento, J. L., and Armstrong, R. A.: Diagnosing the contribution of phytoplankton functional groups to the production and export of particulate organic carbon, $CaCO_3$, and opal from global nutrient and alkalinity distributions, Global Biogeochem. Cy., 20, GB2015, doi:10.1029/2005GB002532, 2006.

Khatiwala, S.: A computational framework for simulation of biogeochemical tracers in the ocean, Deep Sea Research Part I: Oceanographic Research Papers, 53, 1335–1343, doi:10.1016/j.dsr.2006.06.003, 2006.

Khatiwala, S., Visbeck, M., and Cane, M. A.: Accelerated simulation of passive tracers in ocean circulation models, Ocean Model., 9, 51–69, doi:10.1016/j.ocemod.2004.04.002, 2005.

Klaas, C. and Archer, D. E.: Association of sinking organic matter with various types of mineral ballast in the deep sea: implications for the rain ratio, Global Biogeochem. Cy., 16, 1116, doi:10.1029/2001GB001765, 2002.

Kriest, I., Khatiwala, S. and Oschlies, A.: Towards an assessment of simple global marine biogeochemical models of different complexity, Progress in Oceanography, 86, 337–360, doi:10.1016/j.pocean.2010.05.002, 2010.

Kriest, I., Oschlies, A., and Khatiwala, S.: Sensitivity analysis of simple global marine biogeochemical models, Global Biogeochem. Cy., 26, GB2029, doi:10.1029/2011GB004072, 2012.

Kwon, E. Y. and Primeau, F.: Optimization and sensitivity study of a biogeochemistry ocean model using an implicit solver and in situ phosphate data, Global Biogeochem. Cy., 20, GB4009, doi:10.1029/2005GB002631, 2006.

Kwon, E. Y., Primeau, F., and Sarmiento, J. L.: The impact of remineralization depth on the air-sea carbon balance, Nat. Geosci., 2, 630–635, doi:10.1038/ngeo612, 2009.

Lam, P. J., Doney, S. C., and Bishop, J. K. B.: The dynamic ocean biological pump: insights from a global compilation of particulate organic carbon, $CaCO_3$, and opal concentration profiles from the mesopelagic, Global Biogeochem. Cy., 25, GB3009, doi:10.1029/2010GB003868, 2011.

Le Moigne, F. A. C., Sanders, R. J., Villa-Alfageme, M., Martin, A. P., Pabortsava, K., Planquette, H., Morris, P. J., and Thomalla, S. J.: On the proportion of ballast versus non-ballast associated carbon export in the surface ocean, Geophys. Res. Lett., 39, L15610, doi:10.1029/2012GL052980, 2012.

Lutz, M., Caldeira, K., Dunbar, R., and Behrenfeld, M.: Seasonal rhythms of net primary production and particulate organic carbon flux to depth describe the efficiency of biological pump in the global ocean, J. Geophys. Res.-Oceans, 112, C10011, doi:10.1029/2006JC003706, 2007.

Marsay, C. M., Sanders, R. J., Henson, S. A., Pabortsava, K., Achterberg, E. P., and Lampitt, R. S.: Attenuation of sinking particulate organic carbon flux through the mesopelagic ocean, P. Natl. Acad. Sci. USA, 112, 1089–1094, doi:10.1073/pnas.1415311112, 2015.

Martin, J., Knauer, G., Karl, D. M., and Broenkow, W.: VERTEX: carbon cycling in the northeast Pacific, Deep-Sea Res., 43, 267–285, 1987.

Najjar, R. G., Jin, X., Louanchi, F., Aumont, O., Caldeira, K., Doney, S. C., Dutay, J.-C., Follows, M., Gruber, N., Joos, F., Lindsay, K., Maier-Reimer, E., Matear, R. J., Matsumoto, K., Monfray, P., Mouchet, A., Orr, J. C., Plattner, G.-K., Sarmiento, J. L., Schlitzer, R., Slater, R. D., Weirig, M.-F., Yamanaka, Y. and Yool, A.: Impact of circulation on export production, dissolved organic matter, and dissolved oxygen in the ocean: Results from Phase II of the Ocean Carbon-cycle Model Intercomparison Project (OCMIP-2), 21, GB3007, 2007.

Passow, U.: Switching perspectives: do mineral fluxes determine particulate organic carbon fluxes or vice versa?, Geochem. Geophy. Geosy., 5, Q04002, doi:10.1029/2003GC000670, 2004.

Primeau, P.: n the variability of the exponent in the power law depth dependence of {POC} flux estimated from sediment traps, Global Biogeochem. Cy., 21, GB3001, doi:10.1029/2007GB002923, 2007.

Ridgwell, A., Hargreaves, J. C., Edwards, N. R., Annan, J. D., Lenton, T. M., Marsh, R., Yool, A., and Watson, A.: Marine geochemical data assimilation in an efficient Earth System Model of global biogeochemical cycling, Biogeosciences, 4, 87–104, doi:10.5194/bg-4-87-2007, 2007a.

Ridgwell, A., Zondervan, I., Hargreaves, J. C., Bijma, J., and Lenton, T. M.: Assessing the potential long-term increase of oceanic fossil fuel CO_2 uptake due to CO_2-calcification feedback, Biogeosciences, 4, 481–492, doi:10.5194/bg-4-481-2007, 2007b.

Roth, R., Ritz, S. P., and Joos, F.: Burial-nutrient feedbacks amplify the sensitivity of atmospheric carbon dioxide to changes in organic matter remineralisation, Earth Syst. Dynam., 5, 321–343, doi:10.5194/esd-5-321-2014, 2014.

Sarmiento, J., Gruber, N., Brzezinski, M., and Dunne, J.: High-latitude controls of thermocline nutrients and low latitude biological productivity, Nature, 427, 56–60, doi:10.1038/nature02127, 2004.

Sarmiento, J. L., Dunne, J., Gnanadesikan, A., Key, R. M., Matsumoto, K., and Slater, R.: A new estimate of the $CaCO_3$ to organic carbon export ratio, Global Biogeochem. Cy., 16, 54-1–54-12, doi:10.1029/2002GB001919, 2002.

Schlitzer, R.: Carbon export fluxes in the Southern Ocean: results from inverse modeling and comparison with satellite based estimates, Deep-Sea Res. Pt. II, 49, 1623–1644, 2002.

Sonnerup, R. E., Mecking, S., and Bullister, J. L.: Transit time distributions and oxygen utilization rates in the Northeast Pacific Ocean from chlorofluorocarbons and sulfur hexafluoride, Deep-Sea Res. Pt. I, 72, 61–71, doi:10.1016/j.dsr.2012.10.013, 2013.

Stammer, D., Ueyoshi, K., Köhl, A., Large, W. G., Josey, S. A., and Wunsch, C.: Estimating air-sea fluxes of heat, freshwater, and momentum through global ocean data assimilation, J. Geophys. Res.-Oceans, 109, C05023, doi:10.1029/2003JC002082, 2004.

Stanley, R. H. R., Doney, S. C., Jenkins, W. J., and Lott, III, D. E.: Apparent oxygen utilization rates calculated from tritium and helium-3 profiles at the Bermuda Atlantic Time-series Study site, Biogeosciences, 9, 1969–1983, doi:10.5194/bg-9-1969-2012, 2012.

Teng, Y.-C., Primeau, F., Moore, J., Lomas, M., and Martiny, A.: Global-scale variations of the ratios of carbon to phosphorus in exported marine organic matter, Nat. Geosci., 7, 895–898, doi:10.1038/ngeo2303, 2014.

Wilson, J. D., Barker, S., and Ridgwell, A.: Assessment of the spatial variability in particulate organic matter and mineral sinking fluxes in the ocean interior: implications for the ballast hypothesis, Global Biogeochem. Cy., 26, GB4011, doi:10.1029/2012GB004398, 2012.

Yao, X., and Schlitzer, R.: Assimilating water column and satellite data for marine export production estimation, Geoscientific Model Development, 6, 1575–1590, doi:10.5194/gmd-6-1575-2013, 2013.

Zeebe, R. E.: LOSCAR: Long-term Ocean-atmosphere-Sediment CArbon cycle Reservoir Model v2.0.4, Geosci. Model Dev., 5, 149–166, doi:10.5194/gmd-5-149-2012, 2012.

Table 1. Example of using a transport matrix to calculate ~~PO_4~~ PO_4 remineralisation (~~μmol kg^{-1} dt^{-1}~~ µmol kg^{-1} yr^{-1}) in one grid-box from ~~PO_4~~ PO_4 concentrations (~~μmol kg^{-1}~~ µmol kg^{-1}) given in ~~**c**~~ $\boldsymbol{c}$. Grid-boxes, taken from a row of the TM, are arbitrarily numbered, where the 1 is the central grid-box where the calculation is taking place. ~~Coefficients from **A** represent the change in~~ The example shows a ~~tracer due~~ simplified situation where there are 6 neighbouring grid-boxes with their relation to ~~circulation after a single time-step, e~~the central grid-box given by the directions in brackets. ~~g.~~ Each coefficient in the ~~proportion~~ 6 boxes represents the flux of ~~tracer concentration left~~ PO_4 into the central box from that grid-box. The coefficient in the central grid-box ~~1 after one time step is 0.98753~~ for **A** (see Eq.~~(~~ 1)~~). Coefficients from **A-I** are~~ represents the ~~same except now~~ amount of tracer left in the central grid-box ~~1 is equivalent to 1-0.98753~~ after one timestep whilst the coefficient for $\mathbf{A} - \mathbf{I}$ (see Eq.~~(**??** 3)). is~~ the flux out, equal to 0.9816-1. The sum of ~~the~~ coefficients ~~are~~ is shown underneath ~~. The amount in italics is~~ with the estimated remineralisation ~~combining **A-I** and **c**~~ (~~**q** q~~ in Eq.~~(~~ 3) ~~)~~in bold calculated as the sum of the element wise multiplications of $\mathbf{A} - \mathbf{I}$ and $\boldsymbol{c}$.

~~Grid-Box~~ Grid-Box	~~A~~ A	~~A-I~~ (A − I)	~~c~~ c
1 (‘flux out’)	~~0.98753~~ 0.9816	~~-0.01247~~ −0.0184	~~2.42~~ 2.3439
2 (‘north’)	~~-0.00015~~ −0.0007	~~-0.00015~~ −0.0007	~~2.37~~ 2.3430
3 (‘south’)	~~0.01113~~ 0.0086	~~0.01113~~ 0.0086	~~2.42~~ 2.4334
4 (‘east’)	~~0.00002~~ 0.0002	~~0.00002~~ 0.0002	~~2.37~~ 2.3529
5 (‘west’)	~~0.00008~~ 0.0005	~~0.00008~~ 0.0005	~~2.37~~ 2.3615
6 (‘above’)	~~-0.00001~~ 0.0097	~~-0.00001~~ 0.0097	~~2.38~~ 2.4433
7 (‘below’)	~~0.00006~~ 0.0001	~~0.00006~~ 0.0001	~~2.36~~ 2.3369
~~8~~	~~0.00132~~ 1.0000	~~0.00132~~ 0.0000	~~2.41~~ **0.0011**
~~1.00000 -2.38x10^{-7} 1.35x10^{-5}~~ height			

~~Simulations and Experiments used in this Paper.~~ **~~Name Description~~** ~~*Synthetic Datasets* SYN A synthetic PO_4dataset derived from a 10000 year spin-up of GENIE. A corresponding transport matrix is diagnosed. SYN-NODOM As the SYN dataset but with the fraction of DOM exported set to zero. *Experiments* TWIN The synthetic PO_4field is inverted using the TM and compared to the modelled PO_4remineralisation from SYN ERR-DOM Particulate flux curves are estimated from the PO_4 remineralisation rates from the SYN and SYN-NODOM datasets. ERR-OBS The synthetic $PO_4$is perturbed with error estimates from World Ocean Atlas observations ERR-CIRC The synthetic $PO_4$is inverted using 54 TMs diagnosed from a perturbed-physics ensemble.~~

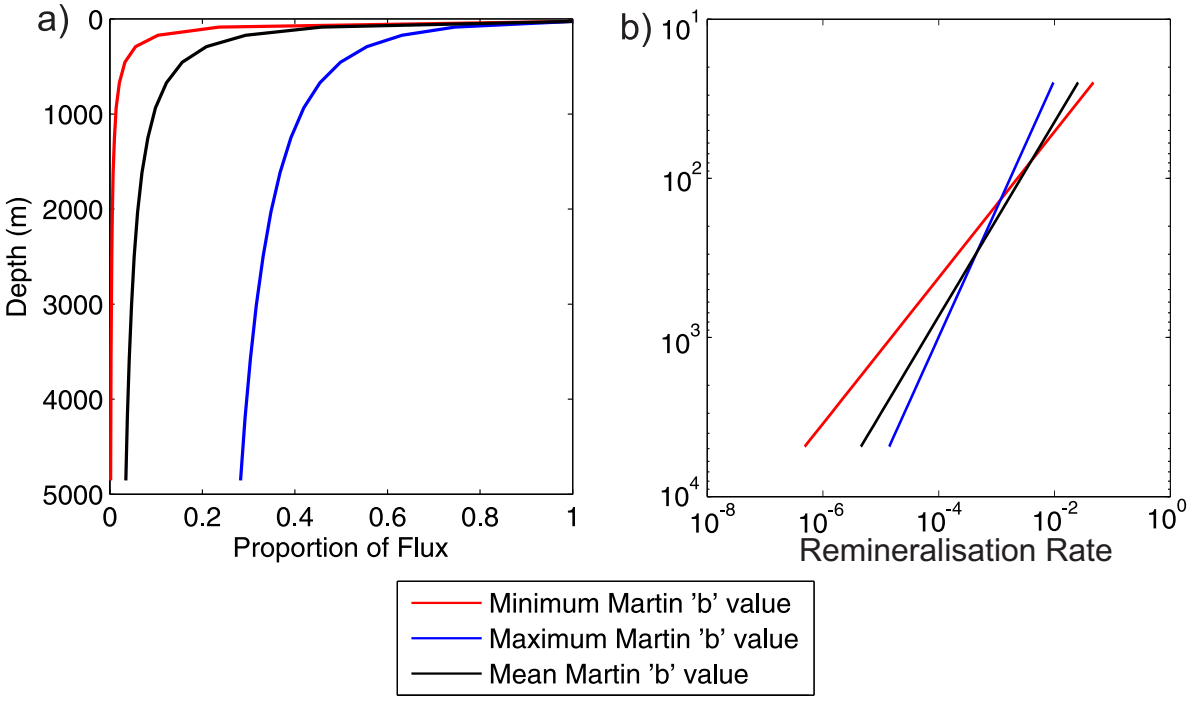

Figure 1. The range of observed Martin Curves and associated remineralisation rate profiles. **(a)** The mean ($b = -0.639$) and global range ($b = -1.18$ to -0.24) of Martin Curves found by Henson et al. (2012) calculated for a unit flux and export depth ($z_0 = 25$m) via $F_z = 1 \cdot \frac{z}{z_0}^{b}$. **(b)** The first derivative of each flux curve in panel **(a)**, equivalent to a vertical profile of organic matter remineralisation calculated as $\frac{\mathrm{d}F_z}{\mathrm{d}z} = \frac{b}{z_0} \cdot \frac{z}{z_0}^{(b-1)}$.

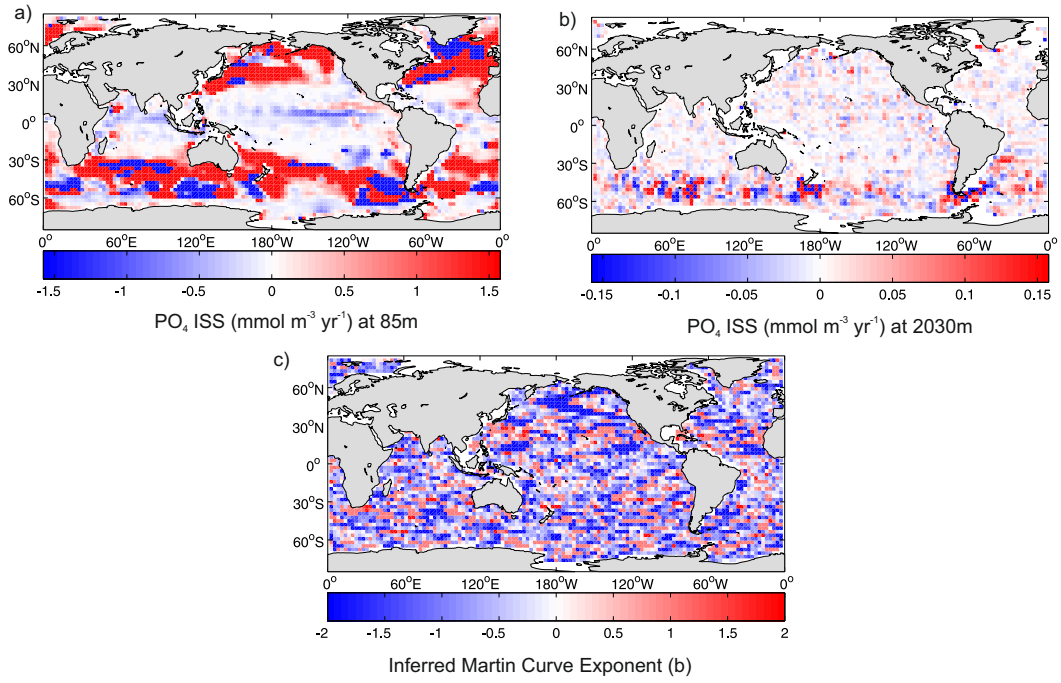

Figure 2. Example of using a GCM transport matrix to estimate PO_4 remineralisation rates. **(a)** The estimated PO_4 remineralisation rates generated using the MIT GCM transport matrix at 85 m and **(b)** 2030 m. **(c)** Power law flux curve exponents (b) inferred from the estimated remineralisation rates by fitting a linear function to the log transformed data as in Fig. 1b.

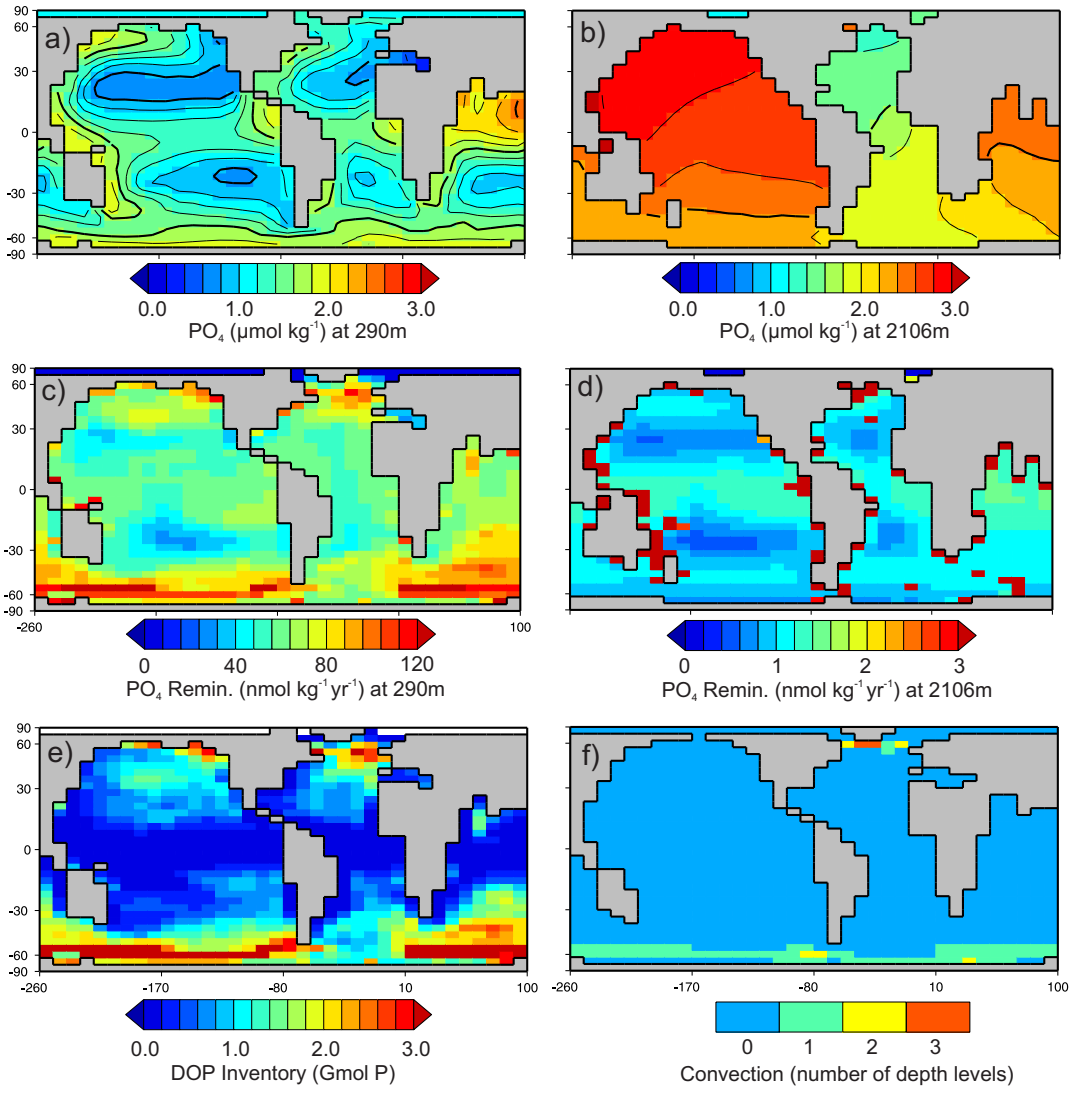
a)
b)
c)
d)
e)
f)
90
60
30
0
-30
-60
-90
-260
-170
-80
10
100
0.0
1.0
2.0
3.0
PO4 (µmol kg-1) at 290m
PO4 (µmol kg-1) at 2106m
0
40
80
120
PO4 Remin. (nmol kg-1 yr-1) at 290m
0
1
2
3
PO4 Remin. (nmol kg-1 yr-1) at 2106m
DOP Inventory (Gmol P)
Convection (number of depth levels)

Figure 3. The synthetic tracer dataset used for transport matrix inversions. **(a)** $[PO_4]$ ($\mu mol\,kg^{-1}$) at 290 m and **(b)** 2106 m. **(c)** The total annual remineralisation flux of PO_4 ($nmol\,kg^{-1}\,yr^{-1}$) at 290 m and **(d)** 2106 m. **(e)** The water column integrated inventory of phosphorus in dissolved organic matter in the ocean interior (mol P). **(f)** A measure of the convection occurring in a water column in one model year (unitless). Higher values indicate the number of vertical levels involved in convection in the model, i.e. stronger convection.

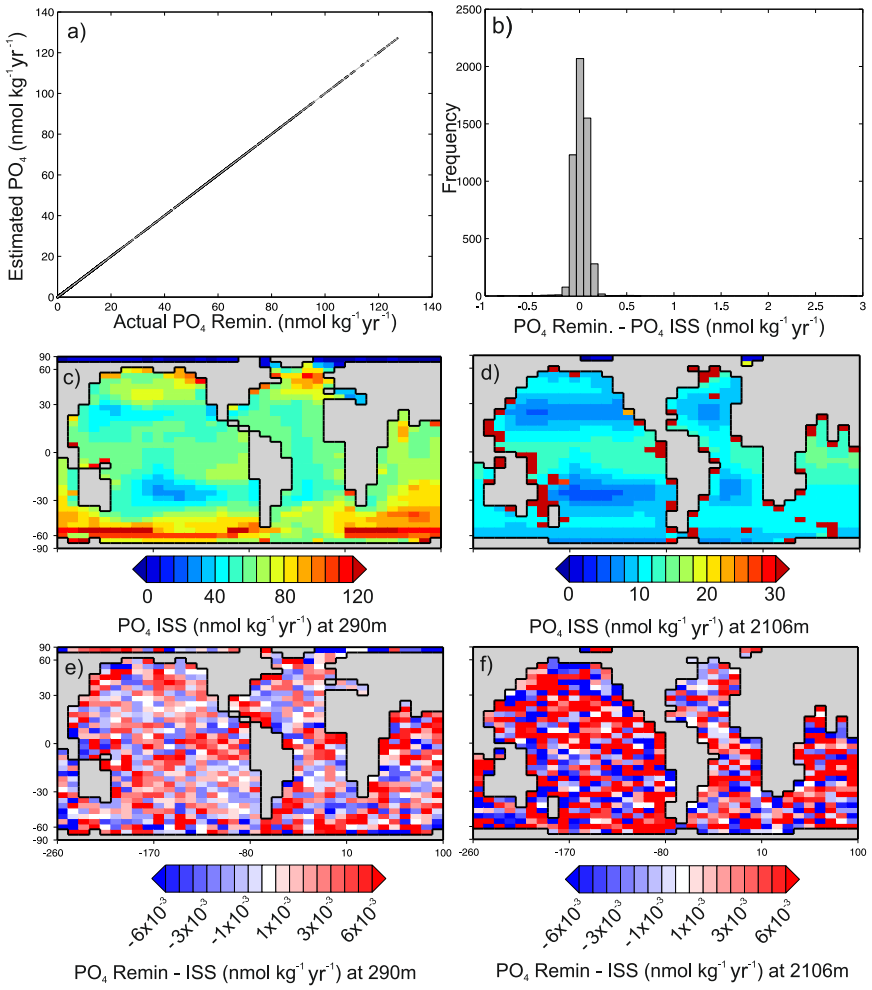

Figure 4. Results from inverting the synthetic dataset with its corresponding transport matrix. **(a)** The interior source/sink estimate for PO_4 when inverting the synthetic $[PO_4]$ field with the corresponding transport matrix vs. the synthetic PO_4 remineralisation with a $1:1$ ratio line, **(b)** the distribution of errors for the PO_4 interior source/sink estimates (50 bins sized 0.15×10^{-5}). **(c)** The interior source/sink estimate for PO_4 at 290 m and **(d)** 2106 m. **(e)** Difference between inverse interior source/sink estimates and the synthetic remineralisation field at 290 m and **(f)** 2106 m.

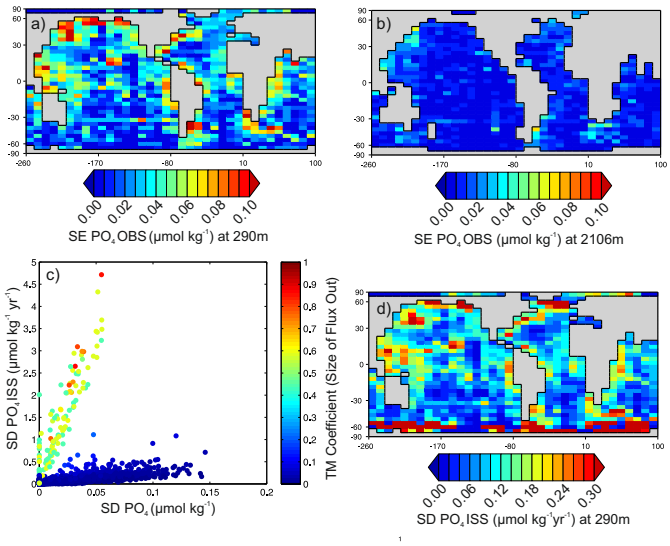

Figure 5. Assessment of the errors arising from the uncertainty in [PO_4] observations. **(a)** The SE of [PO_4] from the World Ocean Atlas 2009 (Garcia et al., 2010) 1° climatology regridded to the GENIE grid at 290 m and **(b)** 2106 m. **(c)** SD of all PO_4 interior source/sink estimates when the synthetic [PO_4] field is randomly perturbed within a normal distribution given by the SE of observations. The colour scale indicates the size of the 'flux out' term where a larger value indicates relatively larger circulation fluxes in that grid-box, **(d)** The SD of [PO_4] ISSs at 290m.

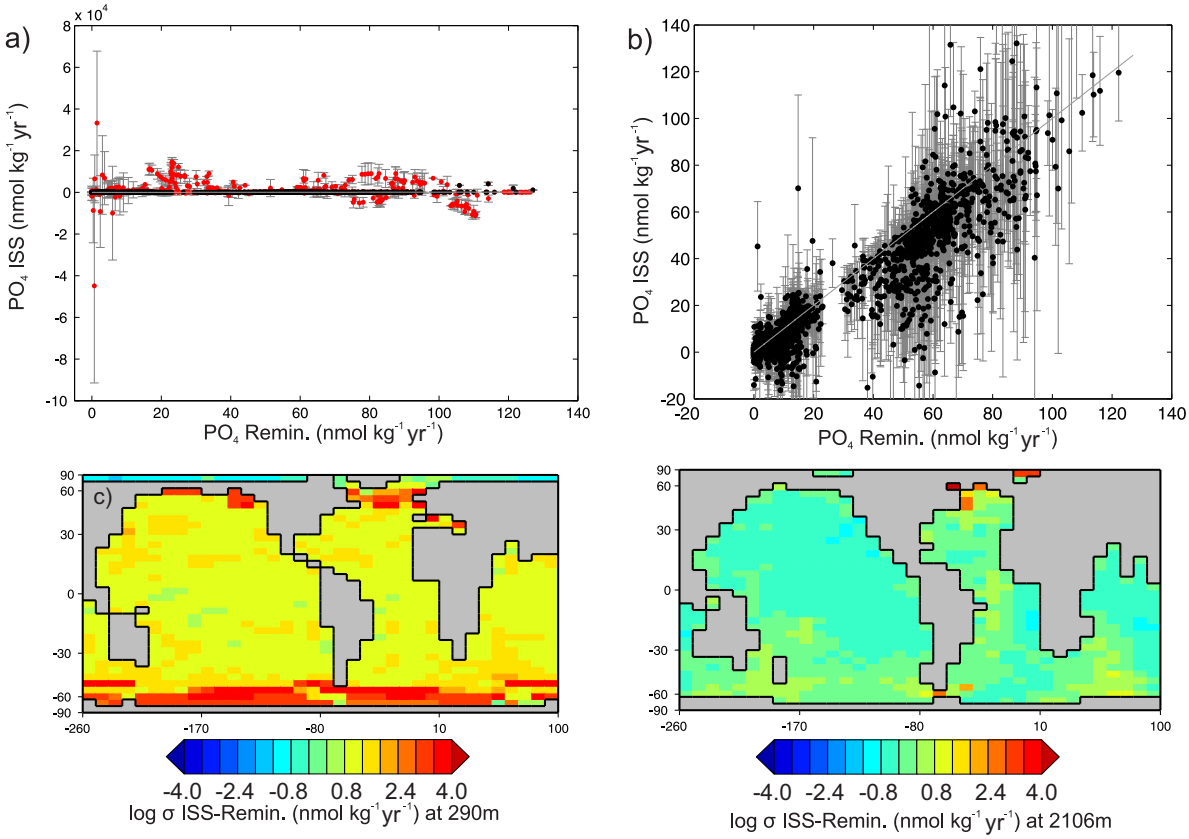

Figure 6. Assessment of error arising from using circulation estimates. **(a)** Comparison of ISS estimates for each grid-box from the 54 ensemble members against the synthetic dataset remineralisation. Error bars are 1 SD around the mean. Red values indicate regions with convection. **(b)** As panel **(a)** but with the red values removed. Note the difference in scale. **(c)** The SD of PO_4 ISS errors (Model – ISS) in $\mu mol\ kg^{-1}\ yr^{-1}$ for 290 m. Values are shown on a log scale. **(d)** As panel **(c)** but at 2106 m.

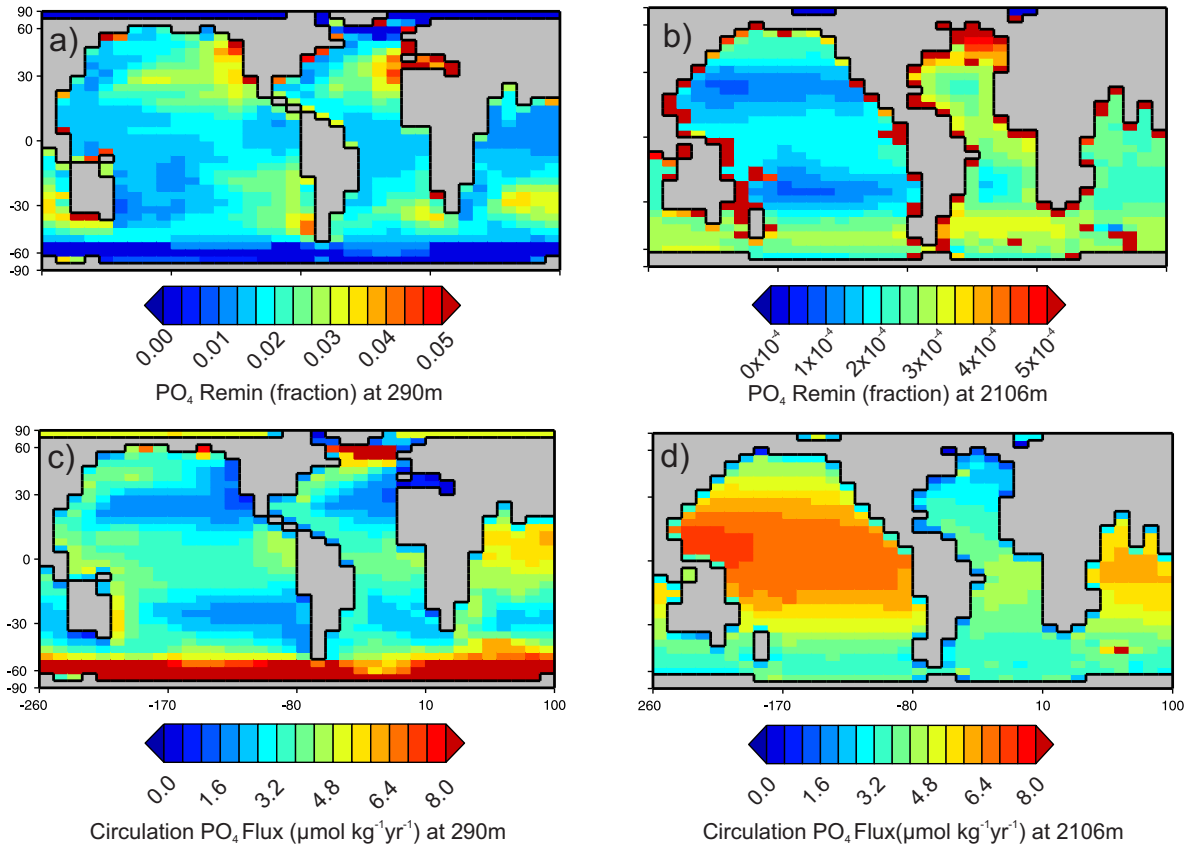

Figure 7. Comparison of inputs of PO_4 from remineralisation and circulation at steady-state. **(a)** PO_4 remineralisation as a proportion of the total PO_4 flux into each grid-box calculated using the synthetic tracer field at 290 m and **(b)** 2106 m. **(c)** The flux of PO_4 into each grid-box from circulation only ($\mu mol\, kg^{-1}\, yr^{-1}$) from the synthetic tracer fields at 290 m and **(d)** 2106 m.

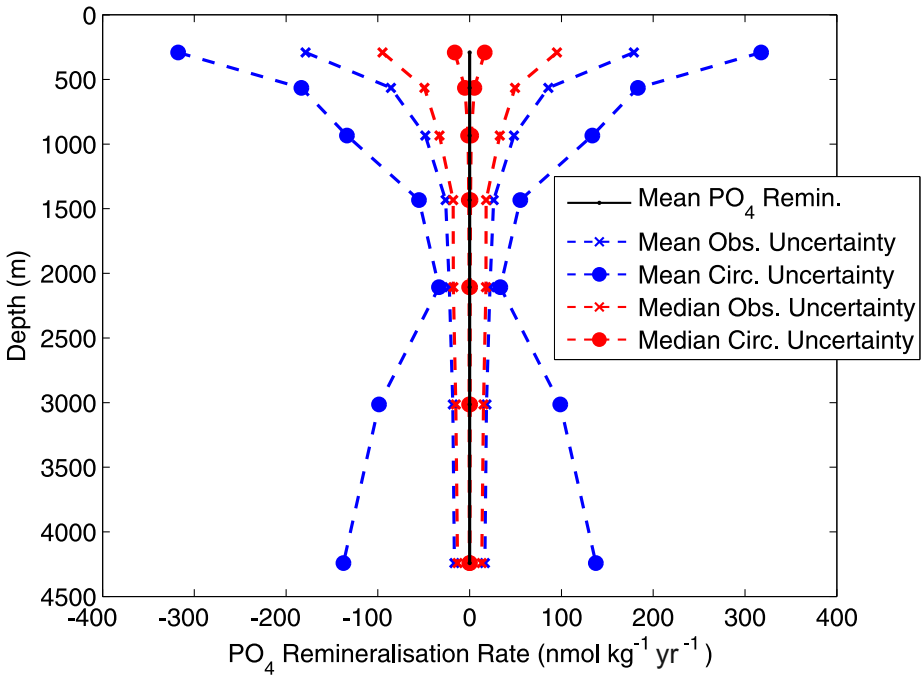

Figure 8. Comparison of error magnitudes when estimating remineralisation rates. The global mean PO_4 remineralisation profile from the synthetic dataset is shown with the plus and minus the mean and median SDs from the ERR-OBS and ERR-CIRC experiments.

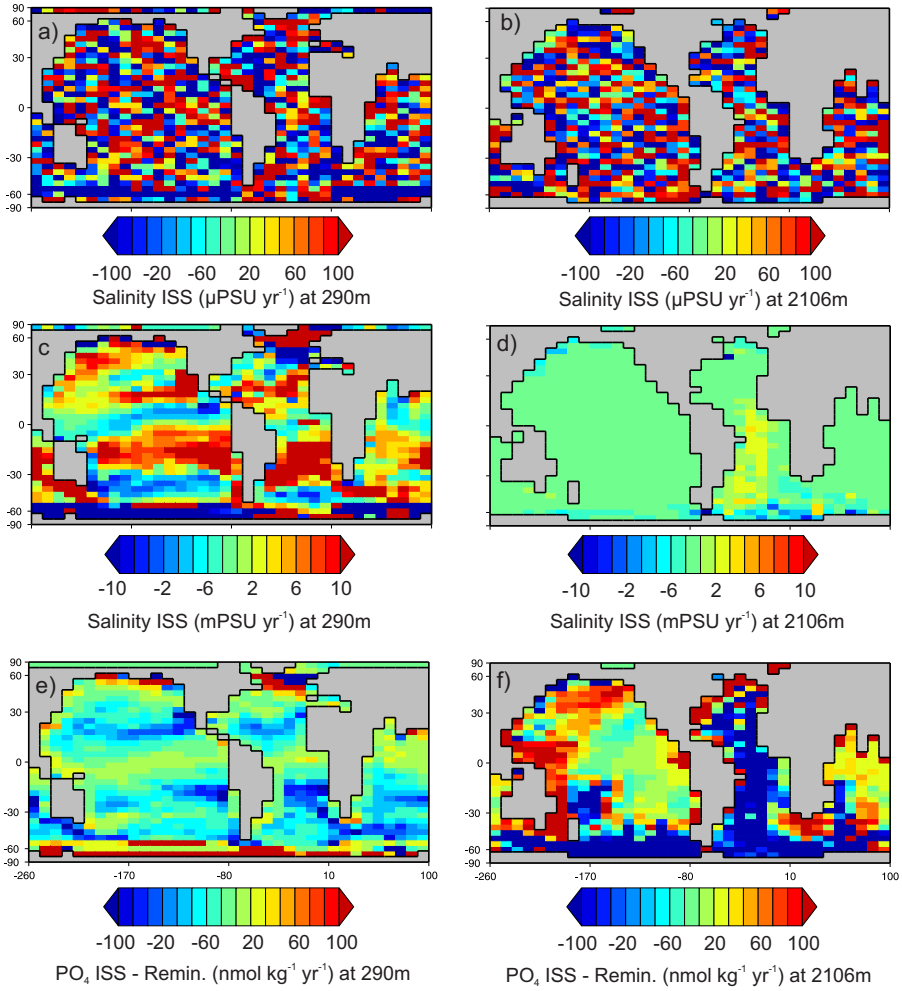

Figure 9. Inversion of salinity as a possible constraint on the uncertainty from using a modelled circulation. **(a)** Inversion of the salinity field from the synthetic dataset using the corresponding transport matrix at 290 m (PSU yr^{-1}) and at **(b)** 2106 m. **(c)** Inversion of the salinity field using a alternative transport matrix from the perturbed-physics ensemble (PSU yr^{-1}) at 290 m and **(d)** 2106 m. **(e)** The error of the synthetic PO_4 ISS ($\mu mol\, kg^{-1}\, yr^{-1}$) (ISS-synthetic) using the same transport matrix in panels **(c,** d) at 290 m and **(f)** 2106 m.

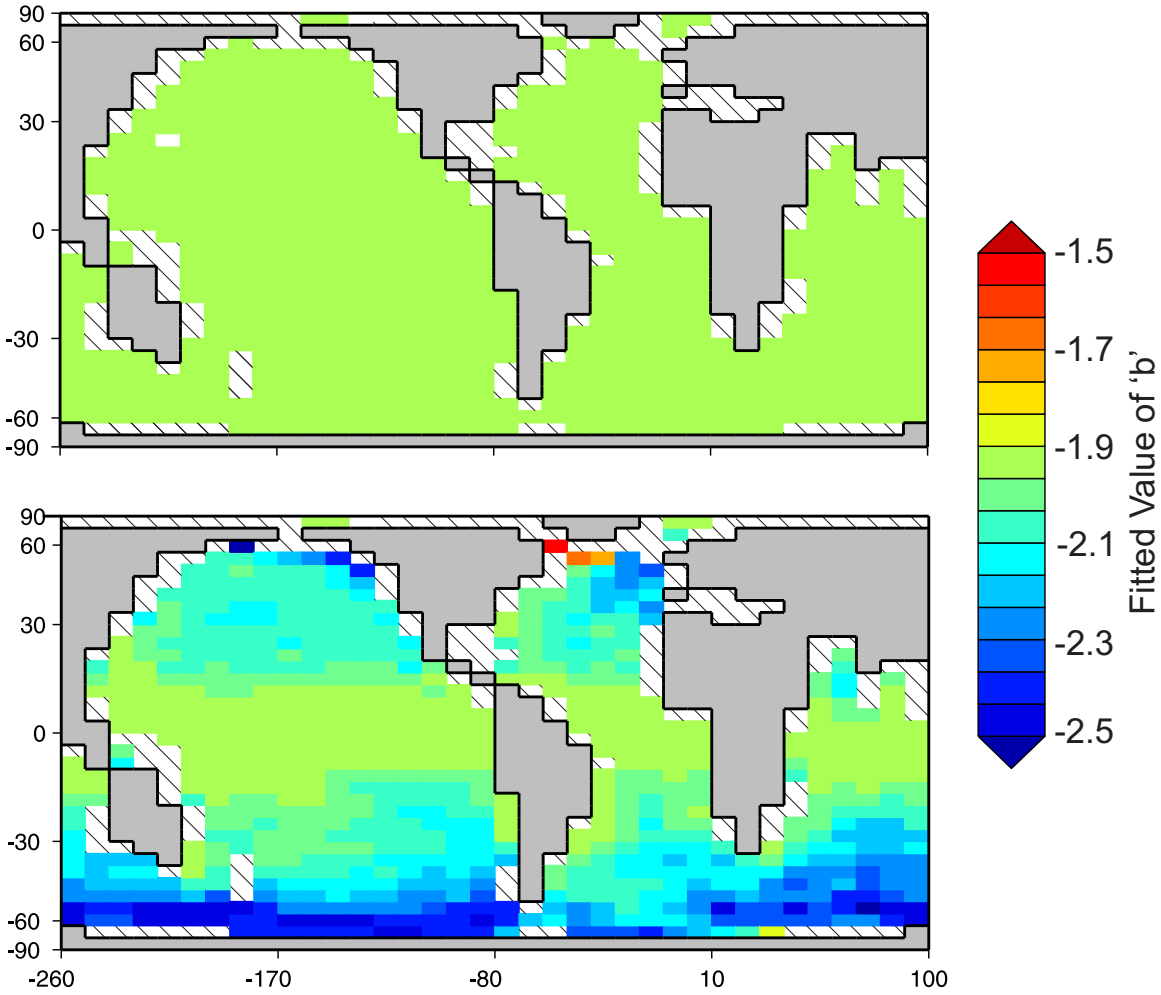

Figure 10. Assessment of the uncertainty associated with dissolved organic matter when inferring flux profiles. Value of the exponent when fitting a power law to the water column remineralisation rates from **(a)** a model with remineralisation from only sinking particulate and **(b)** a model with particulate and dissolved organic matter. A value of -0.858 for the Martin Curve was used in both models. All curves were fitted with an $R^2 > 0.9$. The exponent for the remineralisation curve is equivalent to -0.858 ± 1. More negative values indicate a Martin Curve that predicts shallower remineralisation in the water column. Hatched areas indicate where the water column contained too few boxes to fit a remineralisation curve ($n < 3$).